

Robert Arajärvi

MODELING RADAR PERFORMANCE FOR A SITE-SPECIFIC DIGITAL TWIN

Master's thesis
Faculty of information Technology and Communication Sciences
Examiner: D.Sc.(Tech) Pasi Pertilä
March 2023

ABSTRACT

Robert Arajärvi: Modeling radar performance for a site-specific digital twin
Master's thesis
Tampere University
Electrical Engineering
March 2023

The impact of terrain on the performance of medium and long range surveillance systems must be recognized in order to identify and improve their functionality where necessary. Measuring the exact overall performance of these systems is particularly challenging because there are many factors to consider. Terrain is one of the most significant limiting factors in the ability of ground-based radars to detect targets at long distances.

This study examines the effect diffraction caused by natural obstructions, such as surface shapes and vegetation, has on the site-specific radar systems. The phenomenon may significantly weaken the radio waves, especially when the target is hidden below the visual horizon or in the shadow area. To model the terrain, a terrain model has been created that combines three different sets of terrain information in the direction of the transmitted radar signal.

The diffraction attenuation affecting the digital twin of a radar system was calculated and visualized using a constructed terrain model and two different diffraction models. The use of other diffraction models was also evaluated based on individual circumstances. The resolution of the terrain data used limited the more detailed modeling of the terrain and the use of other diffraction models. However, the methods developed in the study provide a consistent way to determine the magnitude of attenuation and the dominant terrain types of different terrain locations for different propagation paths.

Keywords: digital twin, diffraction modeling, radar, terrain model

The originality of this thesis has been checked using the Turnitin OriginalityCheck service.

TIIVISTELMÄ

Robert Arajärvi: Tutkan asemapaikkakohtaisen suorituskyvyn mallintaminen digitaalisena kakso-

senä

Maisterin tutkinto

Tampereen yliopisto

Sähkötekniikka

Maaliskuu 2023

Maaston vaikutus keski- ja pitkänmatkan valvontatutkajärjestelmien suorituskykyyn on tiedostettava, jotta niiden toimintakyky pystytään tunnistamaan ja tarvittaessa parantamaan. Näiden järjestelmien tarkka kokonais-suorituskyvyn mitaaminen on erityisen haasteellista, sillä huomioitavia asioita on paljon. Maasto on yksi merkittävimmistä rajoittavista tekijöistä maasijoitteisten tutkien kykyyn havaita kohteita pitkällä etäisyyksillä.

Tässä työssä tarkastellaan luonnollisten esteiden, kuten maan pinnan muotojen ja puuston, aiheuttaman diffraktion vaikutusta paikkakohtaiseen tutkajärjestelmään. Ilmiö saattaa aiheuttaa merkittävää vaimennusta radioaalloille etenkin silloin, kun kohde on näkymättömissä visuaalisen horisontin alapuolella eli katvealueella. Maaston yksinkertaistamiseksi lähetettävän tutkasignaalin etenemis-suuntaan on luotu maastomalli, joka yhdistää kolmea eri maastotietoa.

Tutkan digitaalisen kaksoseen aiheutuvan diffraktiovaimennuksen laskemiseen ja visualisointiin käytettiin pääasiassa rakennettua maastomallia, sekä kahta eri diffraktiomallia. Myös muiden diffraktiomallien käyttöä arvioitiin tilannekohtaisesti. Käytettyjen maastoaineistojen resoluutio rajoitti osittain esteiden tarkempaa mallinnusta ja sitä kautta muiden diffraktiomallien hyödyntämistä. Työssä kehitetyt menetelmät tarjoavat silti johdonmukaisen tavan selvittää vaimennuksen suuruuden ja maaston tyyppin dominoivista maastonkohdista eri etenemisreiteille.

Avainsanat: digitaalinen kaksonen, diffraktion mallintaminen, tutka, maastomalli

Tämän julkaisun alkuperäisyys on tarkastettu Turnitin OriginalityCheck -ohjelmalla.

PREFACE

This Master of Science thesis marks the pinnacle of my university education and a significant accomplishment in my academic journey. I am grateful to my colleagues for proposing this fascinating topic. The topic and problems investigated in this thesis were selected and refined together with the Patria Emerging Technology Research (ETR) group.

I am particularly grateful to my thesis supervisors, Pasi Pertilä and Sari Peltonen, for their guidance, support and feedback throughout this project. I want also to extend my genuine appreciation to researchers Juha Jylhä, Minna Väilä and Marja Ruotsalainen for collaborating with me and providing valuable feedback during this thesis.

Finally, I would like to express my gratitude towards my friends and family for their consistent support and encouragement. Their faith in my abilities has been a driving force throughout this challenging yet rewarding experience.

Tampere, 30th March 2023

Robert Arajärvi

CONTENTS

1.	Introduction	1
2.	Radio wave theory	3
2.1	Wave propagation	3
2.2	Radio waves	3
2.3	Fresnel zones	5
2.4	Diffuse reflection and scattering	6
2.5	Diffraction.	6
2.6	Knife-edge diffraction	7
2.7	Bullington diffraction	8
2.8	Fresnel-Kirchhoff diffraction.	9
2.9	Rounded obstacle	10
2.10	Total losses	10
3.	Radar theory	12
3.1	Radar measurements	12
3.1.1	Range measurement	13
3.1.2	Range resolution	13
3.1.3	Signal processing	14
3.1.4	Accuracy of the range measurement	16
3.1.5	Azimuth and elevation measurement	16
3.1.6	Radar equation	18
3.1.7	Bias errors	19
3.2	Performance calculation	20
3.2.1	Detection threshold and probability of detection	20
3.2.2	Limiting factors	21
3.3	Digital twin of radar and its surroundings	21
3.3.1	Path attenuation	22
3.3.2	Terrain model	22
3.3.3	Site-specific radar simulation	24
4.	Proposed methods	26
4.1	Terrain under line-of-sight	26
4.2	Diffraction modeling of radio wave propagation	29
4.3	Summary of methods	30
5.	Results	32
5.1	Case 1	33

5.2 Case 2	34
5.3 Case 3	36
5.4 Case 4	38
5.5 Case 5	39
5.6 Summary of results	41
6. Discussion and conclusion	42

LIST OF SYMBOLS AND ABBREVIATIONS

AER	Azimuth, Elevation, Range
AESA	Active Electronically Scanned Array
AGL	Above Ground Level
AMSL	Above Mean Sea Level
CPI	Coherent Processing Interval
CW radar	Continuos-wave radar
DEM	Digital Elevation Model
EM	Electromagnetic
ESA	European Space Agency
FOM	Figure of Merit
FSPL	Free-Space Path Loss
IEEE	Institute of Electrical and Electronics Engineers
KED	Knife-Edge Diffraction
LCCS	Land Cover Classification System
LOS	Line-of-sight
NLS	National Land Survey of Finland
NN	Nearest Neighbor
OTHR	Over-The-Horizon Radar
PCR	Pulse Compression Ratio
PD	Probability of Detection
PFA	Probability of False Alarm
RCS	Radar Cross-Section
rms	root-mean-square
rss	root-sum-square
SAR	Synthetic Aperture Radar
SNR	Signal to Noise Ratio
TAU	Tampereen yliopisto (engl. Tampere University)

UHF	Ultra High Frequency
VHF	Very High Frequency
WGS84	World Geodetic System, 1984
YPR	Yaw, Pitch, Roll

1. INTRODUCTION

Classical methods for measuring the performance of a radar system include testing its maximum range, which is the farthest distance from which the transmitted signal can still successfully detect a target by receiving its back-reflected echo. This result can only be accurately obtained when the reflectivity of the target is known. When evaluating air surveillance radar performance, other important metrics include the ability to accurately determine the range and velocity of a target, as well as its ability to determine the target's direction. However, traditional methods for measuring a radar's performance, such as those mentioned, are no longer adequate in defining the capabilities of a radar system [1].

The dynamic performance of such systems is challenging to specify and even more difficult to quantify through practical trials. It is particularly challenging to estimate the reliability of a single radar observation. Successfully transmitted, echoed, and received radio signals which originate from the radar are referred to as radar observations. There are many sources of error and other factors that add uncertainty to those signals. Finding those sources and tackling their errors by adding a compensation value is usually the most crucial aspect of making best use of any radar. Poor compensation may lead to bad radar data quality or even into a situation where observations cannot be made in the first place due to an insufficient echo signal.

The total reduction in strength of a radar wave as it propagates is the sum of multiple factors such as terrain, temperature, humidity, and clouds. The radar equation is relatively precise at describing different sources of attenuation. The various atmospheric events that have an impact on the radio wave propagation can be studied and modeled with physics. However, there are also other obstacles. Calculating all the reductive effects on a radar signal, in a changing environment as the target moves, is challenging. Notably, the attenuation caused to radio waves by the terrain is especially arduous to model precisely.

Even the most advanced radars are unable to identify what it is that is blocking the signal path. Signals are echoed from a surface in different volumes depending on both the properties of the surface and the angle at which the signal hits it. The phenomenon where waves meet matter and bend around it is called diffraction. If some obstacle causes large enough diffraction to radio waves, the target behind it will simply not show for the radar. This way attenuation by diffraction causes loss to radar performance. By pin pointing

sources of diffraction, their impact on observations and radar performance can be estimated and better understood. For optimal calculations of diffraction, modeling the terrain and the diffraction sources under the propagation path as closely as possible is the first and most important step. Therefore, a terrain model of some kind is required.

In this work, the motivation was to create a more situation-independent method for modeling diffraction caused by the ground, as some existing models tend to simplify the terrain too much. This type of data preparation and model construction is necessary for the terrain data to be reusable and useful in the future, in situations beyond just determining if an airship is above or below the radar's shadow area. For this purpose, a terrain model was created using three different spatial data materials. Information on terrain height, terrain type and forest height was used for modeling the diffraction of the radar signal.

Three different approaches have been employed to calculate the diffraction caused by the ground to a traveling radar signal. The first used solution for a site-specific radar, over the spherical Earth was the knife-edge model. This classical model assumes obstacle as a wall with infinite width that has a certain height value and which no signal can penetrate. In this model, only the terrain point that causes the most interference to the radar signal is considered as such a wall. In trans-horizon propagation, this might not always be the best way to describe the terrestrial path and therefore the Bullington diffraction model was used. It simplifies more terrain into a single knife-edge by taking into account obstacles that limit visual horizon as viewed from both sides, producing an approximated diffraction loss value as an output. In other words, terrain points with the greatest slope angles from the radar's position and from the target's position are both required. While this solution is a satisfactory approach in many situations where the disposition of the terrain is considered, a more accurate determination for rounded obstacles is also implemented. Rounded and smooth obstacles cause additional loss compared to a sharp ones. Therefore, the so called cylinder model was being used where a cylinder is fit into the shape of dominant terrain point.

In this thesis, the second chapter covers basic concepts on radio wave propagation but also on diffraction and ways for its estimation on obstacles of different nature. In the third chapter, the fundamentals of radar theory are discussed, including factors and phenomena that influence with radar systems. The fourth chapter represents methods for estimating amount of diffraction caused by ground and natural environment on radar signal paths. The fifth chapters shows results of these methods and sixth concludes findings on that.

2. RADIO WAVE THEORY

2.1 Wave propagation

A wave is defined as a propagating dynamic disturbance in physics and in mathematics. Electromagnetic (EM) waves are created due to a periodic change of an electric or a magnetic field. In an EM wave, such as light, the interaction between the electric and magnetic fields allows the wave to be sustained and propagated, as described by Maxwell's equations. In free space, EM waves obey the inverse-square law [2]:

$$I \propto \frac{1}{d^2}, \quad (2.1)$$

which states that the energy intensity, I , of an electromagnetic wave is proportional to the inverse of the square of the distance, d , from the source. At typical distances from a transmitter, the transmitting antenna can typically be approximated as a point source. Doubling the distance of a receiver from a transmitter means that the power density of the radiated wave at that new location is reduced to one-quarter of its previous value. In practice, this rate of diminution varies greatly with different conditions.

2.2 Radio waves

EM waves with the longest wavelengths in the EM spectrum are called radio waves, typically with frequencies of 300 GHz and below. The behavior of radio waves as they travel, or are propagated, into various parts of the atmosphere is called radio propagation. The type of wave propagation is determined by the carrier frequency of a transmitted signal. The frequencies of radar sets today range from about 5 MHz to about 130 GHz [3]. The most common propagation method for Very High Frequency (VHF) waves, ranging from 30–300 MHz, and for wave lengths above them is Line-of-sight (LOS) propagation. The propagation denotes radio waves which travel in a straight line from the transmitter to a receiver. LOS transmission is used for medium-distance radio transmission, such as FM radio, satellite communication, and radar. On the surface of the Earth it is limited to the distance of the visual horizon. The area below the LOS is called shadowed region while the area above it is considered the visible zone as demonstrated in Figure 2.1. If the

receiver is located below the line defined by the horizon, the method of propagation is referred to as trans-horizon.

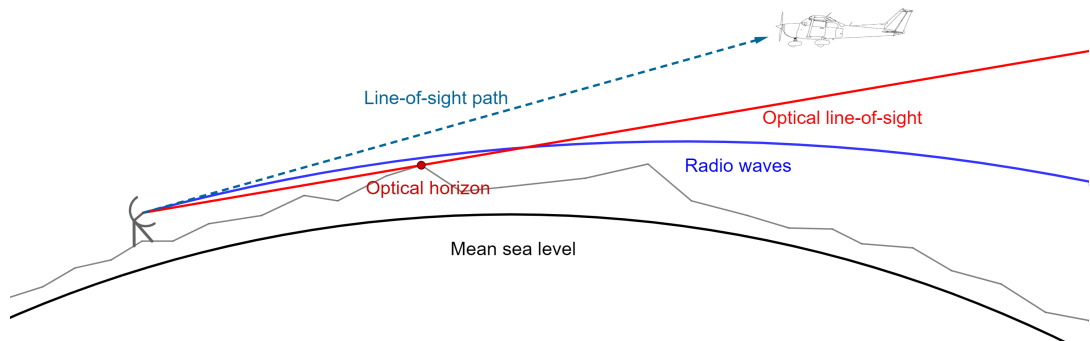


Figure 2.1. Line-of-sight propagation

Radio waves traveling the LOS path through free space are affected by Free-Space Path Loss (FSPL) which is primarily caused by signal energy spreading over larger areas at increased distances from the source. It is defined as the signal attenuation that would be observed if all absorbing, diffracting, obstructing, refracting, scattering, and reflecting influences were sufficiently removed to have no effect on radio propagation. FSPL can be derived from Equation 2.1 when transmitter is considered as an isotropic radiator [4]:

$$L_{fs} = \left(\frac{4 \cdot \pi \cdot d}{\lambda} \right)^2, \quad (2.2)$$

where d is distance from transmitter to receiver in meters and λ is the wavelength in meters. An isotropic radiator is a hypothetical antenna which represents the radio wave source as a point source radiating in every direction with equal energy. It is used in antenna design but cannot exist in reality. For radio applications this equation is more convenient to be used in its decibel format [5]:

$$L_{fs} = 20 \cdot \log_{10} d + 20 \cdot \log_{10} f + 32.4, \quad (2.3)$$

where d is distance in km and f is frequency of radio wave in MHz. Decibels are usually represented by evaluating ten times the base-10 logarithm of the measured power ratio. Electrical field strength is root-power quantity, therefore base-10 logarithm in this equation is evaluated by a factor of twenty.

Uninfluenced radio waves travel in a straight line on the surface of the Earth but as a form of EM radiation, like light waves, they are affected by many phenomena. In the earth's atmosphere, EM waves are generally bent or refracted downward. This reduces the shadow region but causes errors in the measurement of range and altitude simultaneously. The effect of the earth and its surrounding environment also leads to variability and distortion of the radio signal.

2.3 Fresnel zones

A Fresnel zone is one of the infinite number of concentric ellipsoids of revolution that define volumes in the radiation pattern of a circular aperture. These zones are a result of the interaction of waves with the aperture. Radio waves traveling in a straight line from the transmitter to the receiver may commonly meet obstacles near the LOS path. Radio waves reflected off by these objects may arrive out of phase with the signals that travel directly and reduce the power of the received signal. This can be seen in Figure 2.2 where s_r is a reflected signal inside the first Fresnel zone, r_1 is the radius of the first Fresnel zone on the obstacle's location, d_1 is the distance from the transmitter to the obstacle, and d_2 is the distance from the obstacle to the receiver, which is the opposite end of the path. Theoretically, there are infinite amount of Fresnel zones but the first one defines the critical area for an unobstructed LOS. Fading of the received signal can increase significantly if a radius of the first zones becomes blocked more than 40 percent at any point along the path. If 50 percent of the zone is being blocked, signal loss will be 0.5 or 6 dB. This can be illustrated with Fresnel equation 2.6 by defining $\nu = 0$.

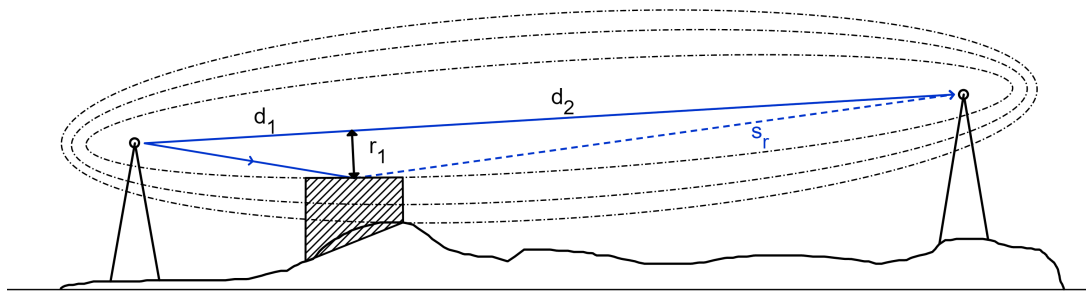


Figure 2.2. Three first Fresnel zones pictured between a transmitter on the left and a receiver on the right.

Fresnel zone radius for radio waves at any point along the line-of-sight path can be calculated [6] as:

$$r_n = \sqrt{\frac{n \cdot d_1 \cdot d_2 \cdot \lambda}{d_1 + d_2}}, \quad (2.4)$$

where d_1 is distance in kilometers between the transmitter and a point of interest, d_2 is distance in kilometers between the point of interest and the receiver, and n is the Fresnel zone number. How much of the Fresnel zone is being blocked by an obstacle does not tell the absolute truth about the proportion of signal fading. The proportion of sent signals detected by receiver, when being in an obstacle's shadow, depends also largely on the shape of the obstacle.

2.4 Diffuse reflection and scattering

EM waves are reflected if they meet an electrically conducting surface. If the matter is a conductor, electric charges are free to move in the matter and then essentially all the wave energy is re-radiated. Radio waves are reflected by objects commensurate with their wavelengths. When waves are reflected from rough terrain, such as natural surfaces, it is called diffuse reflection. It is essentially reflection of waves from a surface in such a way that a ray incident is scattered at many angles. The roughness can be conceived as the variation in surface height since the scattering is specular only over small local regions. This form of reflection is particularly important for the remote sensing of the Earth's surface using Synthetic Aperture Radar (SAR). On the other hand, if the surface is smooth, then the EM wave's angle of reflection equals to its angle of incidence and the reflection is referred as being specular [7].

When EM waves are reflected from small particles in the air, the reflected beam is scattered, or diffused. Distributed water droplets and dust particles diffuse radar energy through absorption, reflection, and scattering so less energy hits its target. The transmitted energy is broken up into many beams that are reflected in all directions. The higher the frequency of the radio wave, the more it is affected by weather conditions such as rain. Although these phenomena should be taken into consideration when calculating total attenuation, for a radio path, diffraction has more potential to cause attenuation to the radio signals.

2.5 Diffraction

Diffraction refers to various phenomena that occur when a wave encounters an object or an opening and consequently travels to places which are not in the direct line-of-sight. It can be explained by Huygens-Fresnel principle, which states that all points on a wavefront can be considered as points for the production of secondary wavelets, which subsequently combined to produce new waves in new directions [8]. When a radio wave encounters an obstacle that is small in comparison to its wavelength, the wave has a natural tendency to bend around it. This bending is called diffraction and it causes a part of the wave energy to divert from the normal LOS path. Another theory that explains diffraction is quantum mechanical theory. Wave functions propose that particles such as photons and electrons can exhibit wave-like behavior and also exhibit diffraction effects.

Although diffracted energy is usually weak, it can be detected by a suitable receiver. The principal effect of diffraction extends the radio range beyond the visible horizon as seen in Figure 2.1. It should be noted that intensity of the radio field is affected not only in the shadow zone but also in the visible part around the tangent ray by diffraction. Most of the time, radio waves encounter one or more separate obstacles and it is useful to estimate

the losses caused by such obstacles. For calculating such loss, it useful to idealize the form of those obstacles.

2.6 Knife-edge diffraction

The EM field in the shadowed region can be calculated by vectorially combining the contributions of all secondary sources described in Section 2.5. This process can be difficult due to the large number of sources involved. However, an approximation can be used that works well in most cases. The Knife-Edge Diffraction (KED) model assumes a single sharp edge with a thickness much smaller than the wavelength that separates the transmitter and receiver. The edge is assumed to have certain height but infinite width. Additionally, no signal can penetrate the obstruction causing some of the rays emitted from the transmitter to not reach the receiver. Above the obstruction, an imaginary plane can be considered in line with it. A point on this plane can be seen as Huygen's secondary source of wavelets, which combine to form waves propagating toward the receiver. This geometry is illustrated in Figure 2.3 where H_s is Huygen's secondary source, Tx is the transmitter, Rx is the receiver, d_1 is distance from the transmitter to the obstacle without height, d_2 is distance from the obstacle to the receiver without height, and h is the obstacle height from the line-of-sight path.

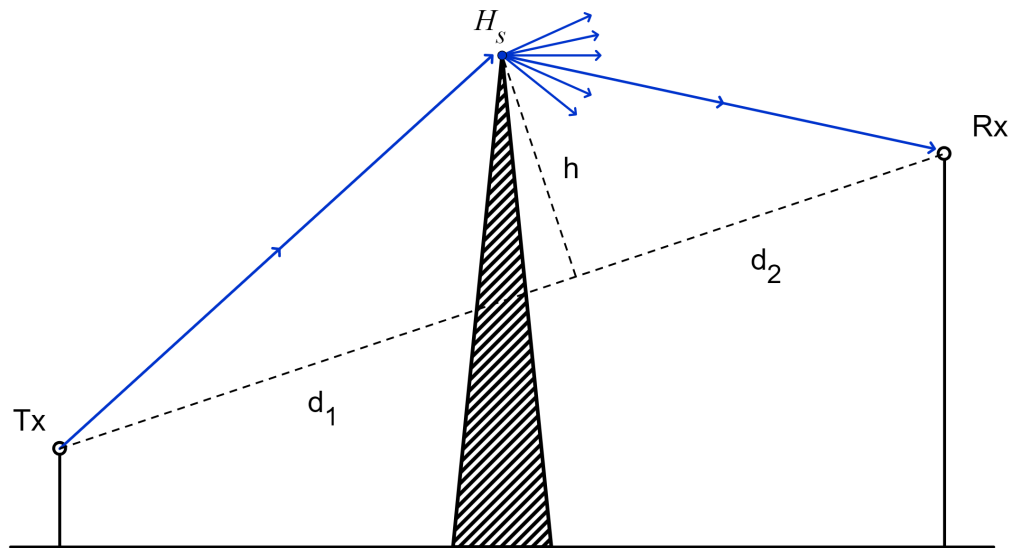


Figure 2.3. Knife-edge diffraction scenario.

The path loss due to diffraction in the knife-edge model is controlled by the Fresnel's diffraction parameter ν , which measures how deep the receiver is within the shadowed region. It is defined [9] as:

$$\nu = h \cdot \sqrt{\frac{0.002}{\lambda} \cdot \left(\frac{1}{d_1} + \frac{1}{d_2}\right)}, \quad (2.5)$$

where h is the height of the obstacle above the line-of-sight in meters and distances d_1 and d_2 are in kilometers. If the obstacle is below the straight path line, then h is negative and if the Fresnel diffraction parameter v is below -1, there is hardly any loss. For the parameter, a value of zero means that the transmitter, receiver and tip of the obstruction are all in line and the electric field strength is reduced by half, or the power is reduced to one fourth of the value without the obstacle.

For calculating the exact diffraction loss, Fresnel cosine and sine integrals have to be evaluated at KED-point but it is computationally expensive. Simpler approximation is developed for $J(v)$, where v is greater than -0.78. The equation for obtaining this value in decibels [10] is:

$$J(v) = 6.9 + 20 \cdot \log_{10} (\sqrt{(\nu - 0.1)^2 + 1} + \nu - 0.1), \quad (2.6)$$

where v is Fresnel parameter from Eq. 2.5. For v values smaller than -0.78, the answer oscillates on both sides of zero with a small margin and therefore it is justified to assume those results as loss being zeros. This model can also be evaluated over multiple obstacles [11]. However, as proposed in [12] the model should be used as a first approach for planning purposes since it is easier to implement in computer code than many other diffraction models. It suggest that, when the accuracy is of paramount importance, preference should be given to the cascaded cylinder model.

2.7 Bullington diffraction

In some trans-horizon scenarios, multiple obstacles may cause significant diffraction to propagating waves. The Bullington model reduces obstacles above the LOS path, from transmitter to receiver, into a single equivalent knife-edge. The location of the edge is the point at which the extended lines joining the transmitter and receiver to their respective dominant obstacles meet. The most dominant obstacle causes a greater angle of elevation, as viewed from the transmitter or from the receiver, when compared to other obstacles in the direction of interest. In Figure 2.4, where the terrain above the LOS is pictured between Tx and Rx, E_b describes the equivalent KED point. Darker colored obstacles are the ones contributing to creating the fictional obstacle in red. Obstacles in lighter gray do not contribute to this diffraction model. The distance to the Bullington point from the transmitter is achieved [13] by:

$$d_b = \frac{h_{rs} - h_{ts} + S_{rm} \cdot d_p}{S_{tm} + S_{rm}}, \quad (2.7)$$

where h_{rs} is height of receiver, h_{ts} is height of transmitter, d_p is the total path distance from transmitter to receiver, S_{rm} is the slope of the straight line path to a receiver's horizon

point and S_{tm} is the slope of the straight line path to a transmitter's horizon point. Heights are in meters Above Mean Sea Level (AMSL) and distances are in kilometers. In the same way, a unit for both horizon slopes is written in meters per kilometers (m/km). With the distance to the Bullington point d_b , the KED parameter associated with the effective knife-edge obstruction can now be evaluated [13] as:

$$\nu_b = \left(h_{ts} + S_{tm}d_b - \frac{h_{ts}(d_p - d_b) + h_{rs}d_b}{d_p} \right) \cdot \sqrt{\frac{0.002}{\lambda \cdot d_b \cdot (d_p - d_b)}} \quad (2.8)$$

Finally the diffraction loss in decibels is achieved with $L_d = J(\nu_b)$ from Eq. 2.6. The Bullington diffraction model is best suited for analyzing trans-horizon propagation. When transmitter's and receiver's horizon are located in the same point, the model yields a result equivalent to that of a normal knife-edge diffraction.

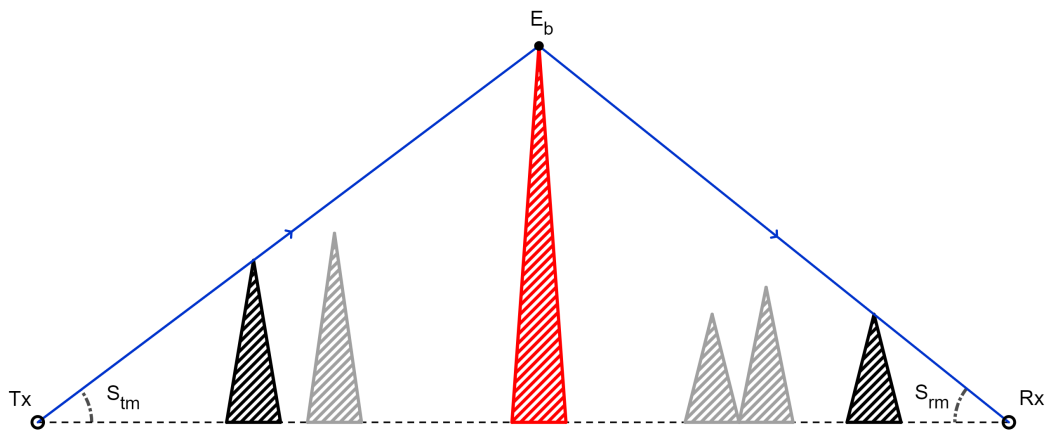


Figure 2.4. Illustration of Bullington diffraction model. The blue line depicts the path of propagation. The darker obstacles contribute to the creation of the imaginary red obstacle, which determines the height of the edge. The light gray obstacles are not involved in modeling the diffraction in this case.

2.8 Fresnel-Kirchhoff diffraction

The Fresnel-Kirchhoff integral is a deterministic, field integral based model for wave propagation. It was first introduced in optics to mathematically formulate diffraction based upon Huygens' principle and was later applied to obtain accurate evaluations of radio communication links to estimate diffraction past obstacles such as irregular terrain but also path loss caused by buildings in urban and suburban areas [14]. Unlike in knife-edge model, here diffraction can also be modeled for a 2-D object which has certain x and y dimension bounds. For a received electric field presented as E_0 , the Fresnel-Kirchhoff

diffraction formula [15] can be represented as:

$$\frac{E_h}{E_0} = 1 - \frac{j}{2} \int_{v_{x0}}^{v_{x1}} \exp(-j\frac{\pi}{2}x^2) dx \int_{v_{y0}}^{v_{y1}} \exp(-j\frac{\pi}{2}y^2) dy \quad (2.9)$$

The integral bounds in Cartesian coordinates are $v_{x[0,1]} = x_{[0,1]}\sqrt{2}/r_1$ and $v_{y[0,1]} = y_{[0,1]}\sqrt{2}/r_1$ where r_1 is radius of the first ($n = 1$) Fresnel zone at the obstacle obtained from Eq. 2.4. The relative magnitude change is $F = |E_h/E_0|$, or, expressed in decibels as $L_d = 20 \cdot \log_{10} F$. For arbitrary terrestrial paths, Fresnel-Kirchhoff theory can be applied although results require repeated numerical calculation. It can closely reproduce diffraction for few exact geometries [16].

2.9 Rounded obstacle

The knife-edge alone is not always the best way to model a dominant obstacle. If the obstacle is characterized as a single rounded or smooth obstacle, it can cause additional loss. To calculate the loss caused by a smooth obstacle, the knife-edge obstacle attenuation should be calculated, and the additional loss term then added. However, the radius of such obstacle's curvature has to be known. The additional loss due to smooth characteristics L_{ex} in decibels can be defined [17] by

$$L_{ex} = 7.5 \cdot \sqrt{\pi \cdot \frac{R}{\lambda}}, \quad (2.10)$$

where R is radius of curvature. Natural shapes of terrain are rarely cylinder-like. Effective radius is estimated by fitting a parabola to the obstacle's profile. In Figure 2.5 such a cylinder, with R representing its effective radius, lays between the transmitter and the receiver. Its size and shape defines a KED point above the obstacle. ITU-R P.526-15 offers solution for calculating cylinder parameters for any multipoint obstacle [10]. However, information on ground topography is required.

2.10 Total losses

To summarize, the total diffraction loss L_d caused by single object can be calculated in decibels [10] as

$$L_d = J(v) + L_{ex}, \quad (2.11)$$

where $J(v)$ is the Fresnel-Kirchhoff loss due to an equivalent knife-edge and L_{ex} is additional loss due to rounded obstacle from Eq. 2.10.

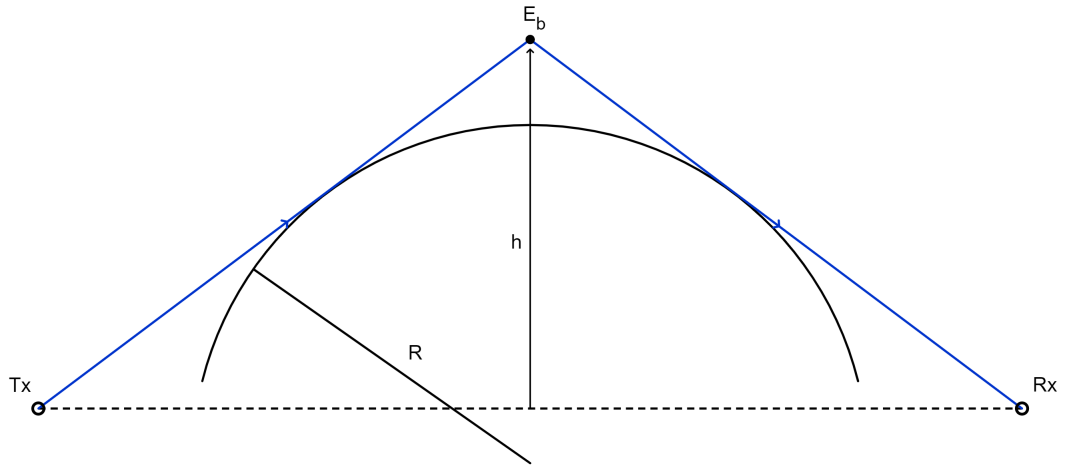


Figure 2.5. Rounded obstacle diffraction.

To obtain the total loss for entire path L_p in decibels the FSPL has to be also considered by

$$L_p = L_f + L_d, \quad (2.12)$$

where L_f is the loss relative to a free space and L_d loss due to a diffraction. The loss relative to free space may be divided into losses of different types, as described by Eq. 2.3.

3. RADAR THEORY

3.1 Radar measurements

A radar is an electromagnetic measuring device that is used for detecting, locating, and tracking objects. It uses radio waves to measure distance, direction, and velocity of an object, usually referred to as a target, by observing the echoes from them. In fact, when a radio wave encounters any matter, a small part of its energy is scattered back and can be then detected by the radar's receiver. Distance measurement is based on calculating the time difference between transmitted and received wave. The velocity, on the other hand, can be determined by measuring the Doppler shift of the echo produced by a moving target. This is done by comparing the frequency of the received signal to the frequency of the transmitted signal. Modern radars also have a capability of imaging and identifying targets. Different radar systems are widely used in all kind of applications thanks to their versatility and the advanced potency of their computational units.

A typical radar consists of a transmitter, an antenna, a receiver, a signal processor, and a display. There are different types of radars and they can be classified according to, for example, physical relationship between the transmitting and receiving antennas, the waveforms they transmit or by their primary mission. Since this thesis is about how ground diffraction affects a radar's performance, the emphasis is placed primarily on monostatic long and medium range air surveillance radar systems operating at Ultra High Frequency (UHF) ranging from 300 MHz to 3 GHz, as well as systems operating in the L and S bands. The Institute of Electrical and Electronics Engineers (IEEE) has designated these bands for the frequency ranges from 1 to 2 GHz and from 2 to 4 GHz, respectively. In air surveillance systems, the antenna is located relatively close to the surface of the earth. In a monostatic radar, unlike in a bistatic radar, the transmitter and receiver share a common antenna. In this work the radar is represented to always face in the direction of the target, although the radio wave beams can also be steered elsewhere with a 360-degree rotating antenna with many air surveillance radars. In contrast, with Active Electronically Scanned Array (AESA) the beam of radio waves can be electronically steered to point in different directions without moving the antenna. Radar beams will be explored more thoroughly in Section 3.1.5.

3.1.1 Range measurement

Measurement of distance is made possible by the properties of radiated electromagnetic energy. Based on the method of transmitting energy, the most popular type of radar is the pulsed radar. The other type of radar is the Continuous-wave radar (CW radar), which detects individual objects based on the Doppler effect. The pulsed radar transmits a short radio pulse with very high pulse power which is focused in one direction only by the directivity of the antenna, and propagates in this given direction with the speed of light. The actual range of a target from the radar along the LOS path is known as the slant range. Since the radar pulse must travel to the target and back before detection, the round trip time has to be divided by two in order to achieve the time for it to go one direction [18]. Therefore the formula for the slant range R in meters can be presented [7, p. 27] as

$$R = \frac{c_0 \cdot t}{2}, \quad (3.1)$$

where c_0 is speed of light and t is the measured runtime in seconds. Due to high speed of radiated energy, radar timing is usually expressed in microseconds. The distances as well as slant ranges are usually expressed in kilometers.

3.1.2 Range resolution

The target resolution of a radar is its ability to distinguish between targets that are very close in either range or bearing. Bearing in radar applications is the determination of the direction. It describes the horizontal angle between the direction of an object and another object or between a line pointed directly at the target and the true north. In the latter case, it is called the "true bearing" which is measured in a clockwise direction from true north. Modern radar sets take on this task, and with the help of GPS satellites, determine the north direction independently. Two different targets can be on the same bearing but at different ranges. In classical radar systems, the degree of range resolution depends mainly on the pulse width of the transmitted pulse. Other factors are the type and size of the target, and the efficiency of the receiver and indicator. For the radar to be able to achieve a good range resolution, an extremely short pulse is required. For example, if the pulse duration is $1\mu s$, the pulse length is approximately 300 meters long. If the distance between two targets on the same bearing is less than half of the pulse width, which means less than 150 meters, the reflected waves from both targets will be combined into one composite wave. Therefore only a one relatively large target will be seen on the radar indicator or display.

However, in pulse radar systems the range resolution of the radar system depends on

the pulse duration instead of a pulse width. Pulse compression is a method for improving the range resolution in those systems. The transmitted pulse is modulated after which correlation is done between the received signal and the transmitted pulse. The ability to compress the pulse depends on the bandwidth of the transmitted pulse. By default, the radar receiver needs at least the same bandwidth to process the full spectrum of the echo signals. Range resolution δR can be calculated [7, p. 785] from the equation

$$\delta R = \frac{c_0}{2 \cdot B}, \quad (3.2)$$

where B is the the bandwidth of the transmitted pulse in Hertz. Pulse compression, or intra-pulse modulation, combines the energetic advantages of very long pulses with the advantages of very short pulses. The method allows very high resolution to be obtained with long pulses. Theoretically a 0.05 m slant range resolution could be achieved with a bandwidth of 1 GHz [3].

The internal modulation of the transmission pulse is carried out to improve the range resolution when the transmission pulse duration is relatively long. A frequency comparison between the transmitted and received signals can be then made in the received echo, allowing for localization of the reflecting object within the pulse. The Pulse Compression Ratio (PCR) is the ratio of the time duration of the uncompressed transmitted pulse to the duration of the compressed pulse. For further calculations, the time-bandwidth product is introduced, the derivation of which results from the ratio of the different resolutions [3] as

$$PCR = \frac{(c_0 \cdot \tau / 2)}{(c_0 / 2B)} = B \cdot \tau, \quad (3.3)$$

where τ is pulse duration in seconds. The range resolution of a pulse modulated radar can be then achieved by multiplying PCR with δR from Equation 3.2.

3.1.3 Signal processing

The signal processor is the component of a radar system that is responsible for distinguishing targets from clutter based on their Doppler content and amplitude characteristics. In electronic systems, particularly in radar systems, clutter refers to unwanted echoes. These echoes may be returned from various sources such as the ground, sea, rain, atmospheric turbulences, and chaff, which is a type of countermeasure used to mislead radar systems. The Doppler content refers to the shift in frequency of the reflected radar signal caused by the movement of the target, while the amplitude characteristics refer to the strength or intensity of the reflected signal. Radar's detector uses these characteristics to filter out unwanted signals and focus on detecting the desired targets. In addition to any clutter that may be present, there will also always be noise present. The

total signal that must be distinguished from the target return is the combination of clutter and noise. Noise filtering will be covered more in Section 3.2.1. The signal processing chain of a radar is illustrated in Figure 3.1.

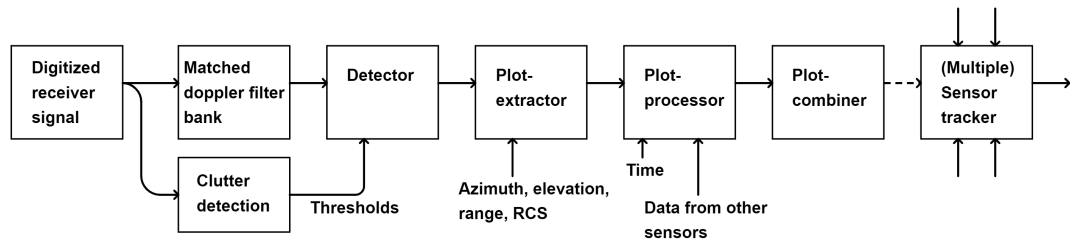


Figure 3.1. A block diagram of radar signal processing chain [3].

As the range from the pulse radar to a target is computed using the time between the transmitted and received pulse, it is necessary to detect the pulse edge in order to maintain its accuracy. Modern radars use matched filter techniques. The receiver in a radar system is equipped with a filter bank designed to detect the received signal at different Doppler velocities. The Doppler velocity refers to the speed and direction at which the target is moving relative to the radar system. The correlation peak of the received signal from the target is used in order to determine the range and Doppler velocity of the target. The Doppler filter bank produces the Doppler spectrum for a target, which can be used for target recognition. For example, when identifying a helicopter, the peak of the signal from the rotor blades and the target's radial velocity can be used to determine the Doppler spectrum peaks. This same effect can also be applied to other air platforms, such as jet engines, by analyzing the frequency shift of the signal reflected from the compressor blades.

Upon receiving the output from the radar detector, the plot extractor's role is to identify and group together threshold crossings that are believed to be from the same target by correlating the hits. The plot extractor can evaluate the energy of a plot based on the distribution of hit amplitudes across the beamwidth. This plot energy parameter can be used to distinguish between different types of targets based on the amount of EM radiation that is scattered back and movement characteristics. The parameter is often passed on to the plot processor for further analysis. The plot processor combines primary plots from different primary radar channels or sources to create a single, most accurate plot. The plot extraction and plot processing elements are the final stage in the primary radar sensor chain. The plot combiner combines primary and secondary radar plots and can include a scan-to-scan correlator to eliminate false or repeated returns. The radar signal processing chain may also include a sensor tracker and a multiple sensor tracker. A sensor tracker combines multiple plots of a target from a single radar sensor into a single track, while a multiple sensor tracker merges tracks from multiple radar sensors to provide a more comprehensive view of the target. The multiple sensor tracker is used to improve

the accuracy and reliability of radar tracking by combining data from various sources.

3.1.4 Accuracy of the range measurement

Range accuracy is the radar's ability to measure the position of a target. The theoretical maximum accuracy with which a distance can be measured depends on the accuracy of the run time measurement. With a pulse radar, the run time is generally measured from the rising edge of the transmit pulse to the rising edge of the echo signal. The accuracy of the distance measurement essentially depends on the noise or rather on the size of the noise in relation to the impulse. This is described by the Signal to Noise Ratio (SNR). Radar measurement error is usually dominated by components dependent on it. For a SNR of considerably higher than 1, the expected range measuring error σ_R can be calculated [3] with the equation

$$\sigma_R \cong \frac{c_0}{2 \cdot B \cdot \sqrt{2 \cdot SNR}}, \quad (3.4)$$

where B is the bandwidth of the radar waveform, and SNR is the signal-to-noise ratio of the received signal from Eq. 3.6. Bandwidth is the difference between the upper and lower cut-off frequencies of the radar receiver in Hertz. The radar receiver must be able to process the signal bandwidth of the backscattered pulse.

3.1.5 Azimuth and elevation measurement

A radar transmits energy in the form of EM waves and if the reflected waves are received again at the place of their origin, there is an obstacle in the propagation direction. The ability of the radar antenna to concentrate transmitted energy in a particular direction is called directivity. An antenna with high directivity is called a directive antenna. By measuring the direction in which the antenna is pointing when the echo is received, azimuth and elevation angles from the radar can be determined. Azimuth, elevation and range are then mapped from the local to the global reference frame by using the knowledge of the orientation and position of the radar. Azimuth angle is defined as the angle parallel to the horizon and north is typically set as zero. Elevation is the angle between the horizontal plane and the line-of-sight and therefore the reference direction is in the direction of the horizon. Elevation angle is positive above the horizon and negative below the horizon. Azimuth, Elevation, Range (AER) location representation is used to describe observation's location based on observation angles and range made by a sensor.

The antennas of most radar systems are designed to radiate energy in a one-directional lobe or beam that can be moved in bearing simply by rotating the antenna. Essentially, this radar beam is just a sector described by the points at which the transmitted power

was reduced by half but which contains nearly 80 percent of all the transmitted energy. The shape of the beam is such that the echo signal strength varies in amplitude as the antenna beam moves across the target. The point of maximum echo is when the beam points directly at the target. This point is determined by the detection circuitry or visually by the radar operator. When energy is directed into a single direction, most antennas will generally have sidelobes in addition to the mainlobe. This is because an antenna's far field radiation pattern is a Fourier Transform of its aperture distribution. The term aperture refers to the physical size of the antenna or, in the case of the radar, the effective that is used to transmit and receive radar signals. The sidelobes of a radar antenna represent unwanted radiation in undesired directions. Although the power density in the sidelobes is typically much lower than that in the main beam, in the worst case scenario, the energy radiated from these directions can be falsely interpreted as a legitimate observation. The illustration of a antenna radiation pattern is shown in Figure 3.2 where the main axis of main lobe of the antenna is G_{max} , as in maximum gain, and θ_{3dB} is the half power beamwidth of the antenna.

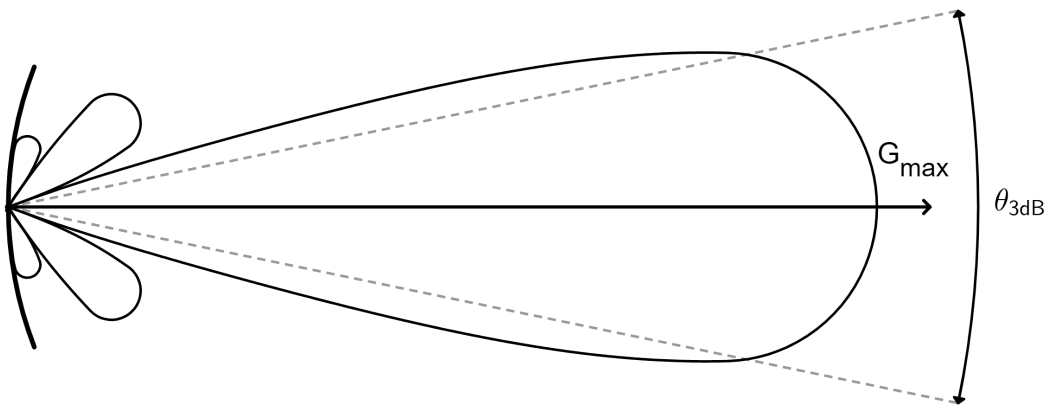


Figure 3.2. A antenna radiation pattern.

As a use-case example, guidance radar systems are based on following the point of maximum echo. A radar antenna is positioned to face the point of maximum signal return and maintained at that position either manually or by automatic tracking circuits. For instance, some older target tracking radars use a conical scan to determine the exact target direction. The idea is to move the radar beam slightly off center from an antenna's central axis and then move the radar antenna toward the area with the strongest echo signal strength [19]. However, soon after it was replaced by monopulse technique which uses additional encoding of the radio signal to provide more accurate directional information. Monopulse radars tackles problems seen in conical scanning radar systems, which can be confused by rapid changes in signal strength. The beam is split into parts and then the two resulting signals are sent out of the antenna in slightly different directions. The reflected signals are then amplified separately and compared to each other when received. The main advantage is that changes in target position or heading will have no effect on

the comparison since the comparison is carried out during one pulse. This method is also used in passive radar systems [20].

With rotating search radar, target angular position may be measured with similar techniques as used in early tracking radars, by finding the center of a series of pulse returns as the antenna sweeps past the target. The measurement accuracy in each angular coordinate is characterized by the root-mean-square (rms) measurement error, σ_A , given by the root-sum-square (rss) of the three error components. One of these components is SNR-dependent random angular measurement error which usually dominates the radar angle errors. It is random, with a standard deviation given for monopulse radar [7, p. 706] by

$$\sigma_{AN} = \frac{\theta}{k_M \cdot \sqrt{2 \cdot SNR}}, \quad (3.5)$$

where θ is the radar beamwidth in the angular coordinate of the measurement, and k_M is the monopulse pattern difference slope. The value of k_M is typically 1.6.

3.1.6 Radar equation

Thermal noise is always present at the radar's receiving antenna. This noise competes with the reflected EM waves from the target that the antenna tries to detect. Also, since the radar's receiver is an electrical device with randomly moving electrons, it generates its own internal thermal noise that competes with the received target signal. The interaction between a monostatic radar and a target can be modeled with the monostatic radar equation. The equation can be formatted into many different forms depending on the use-case. To best describe the correlation of received signal S to background noise N for systems using a modulated pulse it should be written [7, p. 75] as:

$$SNR = \frac{P_t \cdot G_t \cdot G_r \cdot \lambda^2 \cdot \sigma \cdot n_p \cdot PCR}{(4\pi)^3 \cdot R^4 \cdot k \cdot T_s \cdot B \cdot L_s}, \quad (3.6)$$

where P_t is the peak radio frequency power, G_t is the gain of the transmit antenna, G_r is the gain of the receiving antenna, λ is the wavelength of the transmitted signal, σ is the target's Radar Cross-Section (RCS), n_p is the number of Coherent Processing Intervals (CPIs), PCR is the pulse compression ratio from Eq. 3.3, R is the range to the target, k is the Boltzmann's constant, T_s is the system noise temperature, B is the instantaneous bandwidth of the radar, and L_s is the system loss factor. L_s also includes all the loss factors that disturb the EM waves. It bears internal attenuation factors of the radar set on the transmitting and receiving paths L_D , fluctuation losses during the reflection L_f , and atmospheric losses during propagation of the EM waves to and from

the target L_{Atm} . High-frequency components, such as waveguides, filters and also a radome, generate internal losses. For a given radar set this loss is relatively constant and also easily measured. Atmospheric attenuation and reflections at the Earth's surface are permanent influences.

RCS of a reflector is described as a ratio to an idealized reference reflector. The projected area of an equivalent isotropic reflector has an RCS of exactly one square meter. It is measured in units of decibel per square meter (dBsm) and is important quantity in radar performance calculations. RCS of a target depends on the physical geometry of the target, the direction of the illuminating radar, frequency of the radar transmitter, and the electrical properties of the target's surface. It will not change as function of range nor as a function of height, but it will differ fiercely even with a small transition in the illumination angle of the radar with respect to the target's position.

3.1.7 Bias errors

Understanding and minimizing radar biases is crucial part for achieving better quality observations. While radar measurement error is largely dependent on SNR, other error sources to radar systems exist as well. The position and orientation of the radar may easily cause error when local bearing and range measurement are transformed into a global reference frame. A bias offset of 0.01° between the world coordinate system and the local radar coordinate system can cause an error of dozens of meters at a distance of a hundred kilometers. The nature of analog sensors causes the error to vary in each instance of time. Therefore it becomes necessary to perform a real-time analysis of the error. Usually, this means performing an independent error mapping for each type of detection after which compensations are done in X, Y and Z dimensions but also in Yaw, Pitch, Roll (YPR) positions for the target. The range bias is applied to all targets seen by a sensor as a translation. Although, to find absolute range bias, we need more than one sensor.

Some of these errors can be compensated locally but in multi-sensor tracking most of them must be corrected by fusion center where the final decision about target presence is made. In this type of centralized detection model, fusion center is a place where raw observations from sensors are sent to. In track fusion, a common approach to bias error correction is to estimate the bias errors, both offset and scale biases. This is done dynamically by approximating the local measurements from their state estimates and then subtracting them from each other. It gives a measurement of the biases which is independent of the states [21].

3.2 Performance calculation

There are several non-radar dependent factors contributing to the radar measurements that have to be considered when simulating its performance. The ability to receive observations can suffer due to the state of the atmosphere but also because of challenging terrain along terrestrial path. The performance of ground-based radar against low-flying targets has always been limited by land clutter. Modern pulsed radars still encounter difficulties in detecting small targets due to the overwhelming clutter signals and imperfect waveform stability. Although clutter cancellation techniques are implemented, the radar's ability to detect small targets remains severely limited by residual land clutter. Residual clutter refers to the radar reflections that are generated by stationary objects on the ground, such as trees, and buildings [22]. However, there are several metrics that can be used to estimate the performance of a radar in such environments.

3.2.1 Detection threshold and probability of detection

If the signal power of reflected EM waves from the target is assumed to be much greater than the noise power, the target echo signal can be revealed by setting an amplitude threshold. The amplitude threshold is set above the noise level so that every signal greater than that gets detected. However, even with the threshold in place, there is still a chance that noise alone might cross the threshold, giving rise to the possibility of a false alarm. The target-plus-noise signal is a random variable that can drop below the amplitude threshold at any given time, resulting in the probability that it will not be detected. Due to the randomness of these signals, the detection performance of a radar is described through probabilities, the most important being the Probability of Detection (PD). It describes the probability of the target-plus-noise signal exceeding the amplitude threshold. The other important metric used to evaluate the performance is the Probability of False Alarm (PFA), which is the probability for the noise alone spiking above the threshold. Both probabilities increase or decrease together when the threshold is changed. To increase PD while at the same time lowering the probability of false alarm, the target signal power has to be increased relative to the noise power [7].

A radar's detection threshold is decided as a compromise between the desired PD at certain SNR, and on the other hand, the acceptable rate of false detections. If SNR is low, observations will fluctuate up and down more. At the same time, the high SNR can cause clearly higher point in observations. With a high signal to noise ratio, target detection at longer distances becomes easier [23].

3.2.2 Limiting factors

Radio waves are not solely affected by their divergence as they travel or by the diffraction caused by meeting an obstacle. In reality, when these waves are propagated in the Earth's surface or atmosphere, they will also be affected by several other mechanisms, such as magnetic storms, sky noises, sun-spots, but also atmospheric events like rain, clouds, snow, hail, fog, humidity, and wind. Some attenuation due to absorption by atmospheric gases, mostly oxygen and water vapor, is always present and should be included in the calculation of total propagation loss at frequencies above about 10 GHz. Although the rainfall affects propagation only at frequencies above 5 GHz in free space, it is found to affect the propagation even at low frequencies of VHF and UHF bands within the forest environment due to the accumulated rain water on the foliage medium [24].

The target is challenging to detect when an obstacle in the path of propagation blocks the direct LOS path. A rounded surface, like the top of a grassy hill, for example, can obliterate the signal. On the other hand, if the obstacle's profile is sharp, like a forested or rocky terrain top, some portion of the wavefront could be diffracted around or over the obstacle [6]. Trans-horizon propagation mechanism occurs over paths extending beyond the normal radio horizon. For frequencies above 30 MHz two permanent trans-horizon propagation mechanisms are tropospheric scatter and diffraction. Just beyond the horizon, the diffracted field has a rapid exponential decay, of 1 dB/km at frequency of 1 GHz, while the scattered field decay is around 0.1 dB/km [12]. As a result, PD will likely decrease too much for reliable results. However, Over-The-Horizon Radar (OTHR) systems are being used to overcome the LOS limitation caused by the Earth's curvature. They use either surface-wave propagation or sky-wave propagation [25].

3.3 Digital twin of radar and its surroundings

A digital twin is a virtual representation of a real-world physical system or process that serves as its digital counterpart for practical purposes. The difference between a digital twin and a simulation can be seen as a matter of scale. A simulation typically studies one particular process, whereas a digital twin can, by itself, run any number of useful simulations in order to study multiple processes [26]. Perhaps an even more valuable feature is that digital twins can be used to predict a system's future behavior. Being able to predict the capabilities of a radar can be extremely useful and cost-effective, but it can also improve the maturity of the operational radar processing [27]. Simulation of the signal propagation path and the surrounding terrain, in the direction which the signal is traveling, are both vital factors for a digital twin of a ground-based radar system.

3.3.1 Path attenuation

When an obstacle is in the direct path, the radio wave can be detected at the radar receiver either by passing through the obstacles and suffering related attenuation, or by using diffraction mechanism in a way that the waves encounter obstacle edges and penetrate or bend to the shadow region behind the obstacle. If the beamwidth of the transmitter antenna is wide as in sectoral or isotropic antennas, the diffraction phenomenon is the dominant one for two reasons. First, the transmission power is identical for different paths including straight and diffracted paths. Second, the high thickness of natural obstacles in comparison to the wavelength causes high loss for straight path. In LOS radar transmission with directional antennas at high frequencies, the diffraction mechanism is not applicable. Taking into account the obstruction loss is therefore a better approach in a case where the obstacle thickness is not too high in compared to the wave penetration depth [17]. The reliability of radar performance suffers especially when taking observations from lower altitudes since attenuation due to natural obstacles leads to greater diffraction.

The loss caused by natural obstacles has to be acknowledged and calculated. Terrestrial parameters are for instance, mountains, forests and different of water. Forests and other green areas are dominant on the surface of the Earth but their diffraction is not similar to diffraction caused by the ground itself. The loss due to vegetation coverage and especially due to forests is considerable in terrestrial communications. Its effects are significant for point-to-area wireless systems which more or less corresponds to a ground based radar's use-cases. Due to these complicated conditions it is quite challenging to provide a straightforward solution to this problem, let alone a closed form equation. Some solutions are provided based on practical measurements and field experiments like one based on ITU-R P.833-10 [28]. Vegetation near the sensor site has more effect on radar performance than e.g. trees much further away since beam is directed at higher altitudes. This can be countered by chopping down some trees near the sensor. This might lower the radar's visual horizon in the direction of the chopped trees. However, for some sites and directions it should be evaluated if that actually reduces attenuation to the signal enough.

3.3.2 Terrain model

The geospatial information used for creating an artificial radar environment in our terrain model, are Digital Elevation Model (DEM), forest height map, and land cover material. DEM is a numerical representation of the bare ground topographic surface of the Earth excluding trees, buildings, and any other surface objects. It describes ground heights from mean sea level with a grid size of 17.5 meters. Area taken as an example in this section is from 60°98' to 62°03' North and from 23°13' to 24°00' East in the World Geodetic System,

1984 (WGS84). The graphic (a) in Figure 3.3 shows a raster map based on used DEM data where the lowest terrain is represented with dark blue and the higher the terrain, the lighter the shade of blue is. Margin of error in height values in this data is 1.4 meters. This material does not include separate geological objects, such as glacial erratic, or man-made structures. The forest height model shows maximum height of trees with a pixel resolution of 25 meters. This data can be seen from graphic (b) in Figure 3.3 where dark blue describes areas without trees and various shades of green indicate areas with different maximum height of trees and vegetation. There is not much variety in the shades of green since woods are usually dominated by the same tree species and they have certain heights they grow into. These height data materials originate from National Land Survey of Finland (NLS)'s open database which brings together this kind of spatial data in many resolutions [29]. For instance, terrain height data is also available in smaller grid sizes of 10 and 2 meters. DEM data is being updated by NLS by utilizing laser scanning technique in case the terrain is being transformed, commonly due to construction work or other such operations.

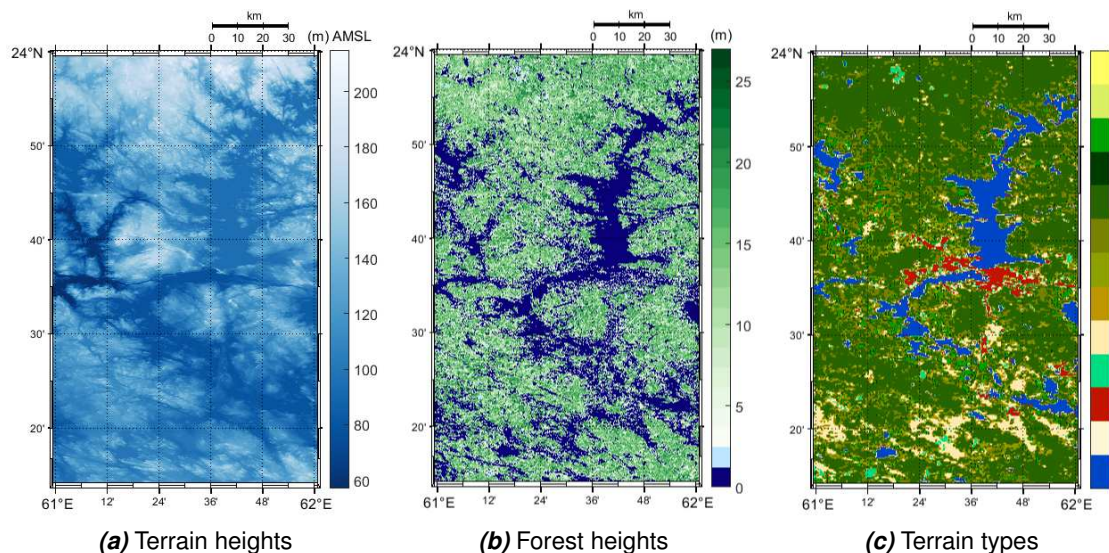


Figure 3.3. Raster maps of all three geo-materials

Land cover material describes the usage of the land type in the area it covers. If there is a certain type of forest covering the land mass, it is represented with a certain value, or when a land coverage is mainly urban, a different value is assigned to it. Global terrain data used in this work originates from the year 2009 and has a grid size of 220 meters. It handles 22 different terrain types as their own, which are based on United Nations' Land Cover Classification System (LCCS). For instance, the value 190 refers to a man-made environment where over half of the area is urban. This can be seen from graphic (c) in Figure 3.3 where urban areas are in red, water is marked in as blue and several shades of darker green indicate forests. For each value in the 2-D map matrix there is a dedicated RGB color value to represent a certain terrain type as shown in Table 3.4. The data is a

part of European Space Agency (ESA)'s GlobCover project [30].

Both DEM and forest height data sets have been used in radar shadow calculations before. However, especially for calculating diffraction, the land cover material might be useful in many applications. The biggest contributor to diffraction can differ and might not always be a tree or a hill. A combined terrain model that includes information about these three materials provides a comprehensive understanding of the terrain and obstacles that may affect the radar beam.

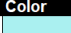



















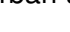
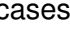

Value	Label	Color
11	Post-flooding or irrigated croplands (or aquatic)	
14	Rainfed croplands	
20	Mosaic cropland (50-70%) / vegetation (grassland/shrubland/forest) (20-50%)	
30	Mosaic vegetation (grassland/shrubland/forest) (50-70%) / cropland (20-50%)	
40	Closed to open (>15%) broadleaved evergreen or semi-deciduous forest (>5m)	
50	Closed (>40%) broadleaved deciduous forest (>5m)	
60	Open (15-40%) broadleaved deciduous forest/woodland (>5m)	
70	Closed (>40%) needleleaved evergreen forest (>5m)	
90	Open (15-40%) needleleaved deciduous or evergreen forest (>5m)	
100	Closed to open (>15%) mixed broadleaved and needleleaved forest (>5m)	
110	Mosaic forest or shrubland (50-70%) / grassland (20-50%)	
120	Mosaic grassland (50-70%) / forest or shrubland (20-50%)	
130	Closed to open (>15%) (broadleaved or needleleaved, evergreen or deciduous) shrubland (<5m)	
140	Closed to open (>15%) herbaceous vegetation (grassland, savannas or lichens/mosses)	
150	Sparse (<15%) vegetation	
160	Closed to open (>15%) broadleaved forest regularly flooded (semi-permanently or temporarily) - Fresh or brackish water	
170	Closed (>40%) broadleaved forest or shrubland permanently flooded - Saline or brackish water	
180	Closed to open (>15%) grassland or woody vegetation on regularly flooded or waterlogged soil - Fresh, brackish or saline water	
190	Artificial surfaces and associated areas (Urban areas >50%)	
200	Bare areas	
210	Water bodies	
220	Permanent snow and ice	
230	No data (burnt areas, clouds,...)	

Figure 3.4. Terrain types and their corresponding colors [30].

Radars, particularly surveillance radars, are rarely placed in close proximity to urban areas or tall buildings due to various reasons. As such, this work does not deal with cases of radar beam interfering with a man-made structure like apartment buildings or wind mills. Apart from this, there is a growing interest in studying diffraction caused by man-made structures due to the increasing amount of telecommunication infrastructure in urban areas. In terms of individual buildings and objects of distinct shape, the Fresnel-Kirchhoff diffraction formula can be applied to model obstacles as 2-D blocks with specific heights and widths 2.8.

3.3.3 Site-specific radar simulation

A digital twin model of a radar system requires foremost its location in a global reference frame but also other parameters depending on what extent it is required to be modeled and what is measured. The most vital information for calculating the radar's performance is the antenna's position, the direction the pulse beams are pointed, and the frequency of the transmitted signal. By acknowledging these factors, the position of each terrain point with respect to the antenna's location, and furthermore how they intervene with the radar signal, can be simulated.

Refractive properties of the earth's atmosphere, as represented in Section 2.4, might

cause the path to bend slightly toward or away from the surface of the Earth. To allow for a straight line path of propagation, a correction factor is applied to the earth's radius. It increases or decreases the surface curvature to compensate for the refracted path. Propagation models utilize a standard atmosphere where the correction factor, or k-factor, is defined as 1.33. A corrected radius is called the effective earth radius. The positive height of surface curvature due to the the effective earth radius h_{ER} in meters at certain point along the path of propagation can be approximated [6] by

$$h_{ER} = \frac{d_1 \cdot d_2}{12.74 \cdot k}, \quad (3.7)$$

where distances d_1 and d_2 are in kilometers and k is the atmospheric correction factor. Previously in this work the point to which diffraction is calculated has been represented as a classical receiver on the ground. In radar applications the point of interest, or target, is always located above trees and most of the time several hundred meters above the surface depending on the type of flying platform.

4. PROPOSED METHODS

In this work, diffraction loss was calculated for the terrain's obstacles between the radar and the target using three models: knife-edge, Bullington, and rounded obstacle model. However, the first two models are mainly presented as the focus of the evaluation. The radar is modeled as a digital twin of ground-based air surveillance radar whose capability is evaluated based on the diffraction loss of its signal at various heights. In these methods, the height values are given in terms of their elevation Above Mean Sea Level (AMSL). Creating a terrain elevation profile for a path of propagating radar signal is described in Section 4.1. Section 4.2 outlines the main principles for determining the appropriate diffraction model based on the terrain features under the LOS path, such as the elevation profile.

4.1 Terrain under line-of-sight

Although in some short distance cases it is reasonable to assume that the direct path of propagation follows a straight line, in reality this is not the case. A curved radio propagation path vertically affects the relationship between a radar signal and a terrain's obstacles. However, the location of obstacles in a horizontal plane must be known first, making the determination of terrain points under the propagation path more challenging. For this problem, an algorithm that collects the required terrain information under the propagation path was designed, and implemented in Matlab. The input data for this algorithm consisted of geospatial data materials described in Section 3.3.2. The other function inputs were radar and target locations, radar transmitter's height above the ground level, target's height AMSL, Nearest Neighbor (NN) value and step size. Locations were given as ETRS-TM35FIN coordinates, which is the Finnish projected coordinate reference system [31]. These coordinates define the start and the end point for the LOS path. Required parameters for a site-specific radar system are better defined in section 3.3.3.

At first, the target's AER position is acquired from the radar's direction. Azimuth and elevation angles are then used as constants to calculate coordinates along the LOS path to the target. Starting from the radar's location, every step coordinate on the path is achieved by traveling into the direction determined by those constant angles and with a range determined by the step size. Coordinates of the height map pixels' centers are

Algorithm 1 Data mapping algorithm

Input: azTreshold = 10, NN = 1, steps = [0,50,100,150...], azMap = m x n matrix, rMap = m x n matrix, HeightMap = m x n matrix

Output: outStruct

```

1: function MAPPING(azTarget, azTreshold, NN, Steps, azMap, rMap, HeightMap)
2:   azDiffs = CalcAngleDifferences(azMap, azTarget)
3:   ixsClose = FindIndices(azDiffs < azTreshold)
4:   ixsDiscretized = Discretize(rMap(IxsClose), steps)
5:   for each index i in steps do
6:     pixels = ixsRDiscretized(i)
7:     pInds = ixsClose(pixels)
8:     stepInfo = [azDiffs(pInds)', rMap(pInds)', HeightMap(pInds)', ...]
9:     stepInfo = Sortrows(stepInfo, '1', ascend)
10:    outStruct[i] = stepInfo(1 : NN, :)
11:  end for
12:  return outStruct
13: end function

```

determined by relative pixel index transition with respect to map's corner coordinates. With these coordinates, the AER location of each pixel is calculated in the same way as target's AER location. Subsequently, the azimuth, elevation, and range for each pixel's center can be defined with respect to the radar, resulting in matrices of eMap, azMap and rMap. The right pixels along the LOS path are acquired from these matrices by mapping. Principle of pixel mapping can be seen in Algorithm 1. Pixels that are too far away in their direction of azimuth are factored out. Differences between the azimuth of the target, azTarget, and the azimuths of the pixels in azMap are calculated. These azimuth differences, azDiffs, are then compared with the azimuth threshold, azTreshold, and pixels with a greater azimuth difference are left out. The remaining ones are discretized by their range values into step size counterparts. An azimuth threshold of 10 degrees is used in this work to crop out the furthest pixels. Although this means that there are more pixels within the same range of azimuth further away, its main purpose is to speed up the discretization. With a step size of fifty meters every terrain height pixel with a range value between 25 and 75 meters would belong to the first group and pixels with range value from 75 to 125 meters would belong to the next group and so forth.

Once pixels are categorized, they are sorted by their azimuth difference value inside each range group. The nearest pixel in every group is the one that has the smallest azimuth difference with the target's azimuth direction angle. The NN value specifies how many nearest pixels are being picked inside each step group. For instance, if the step size is fifty meters and the NN value is 1, it means that after every 50 meters traveled, the data is collected only from the nearest map pixel. A visual presentation of this mapping can be seen in Figure 4.1 where dashed lines are drawn from the map pixels with the smallest azimuth difference into corresponding locations on the path after each step. Tx indicates

the radar's location and Rx the target's location.

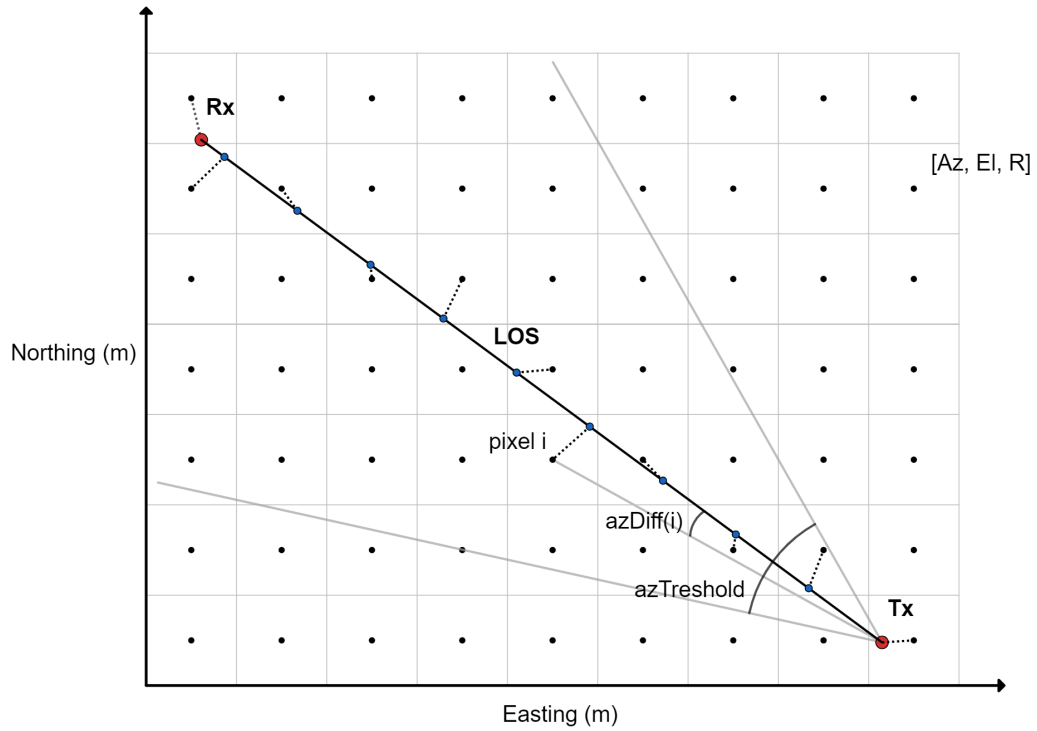


Figure 4.1. Height map pixel mapping with NN value of 1. Each grid point corresponds the center of a height map pixel.

Upon the collection of terrain data along the propagation path, the next step is to determine the relative position for each step in order to indicate radar's visual horizon. With combined height data, slope S_i from radar antenna to individual mapped terrain point under LOS is calculated by dividing relative terrain height by earth distance

$$S_i = \frac{h_i + h_{er} - h_{ts}}{d_i}, \quad (4.1)$$

where h_i is the combined height of ground and trees in meters, h_{er} is earth's bulge from Eq. 3.7 in meters, d_i is earth path distance from antenna to terrain point in kilometers, and i denotes a terrain point associated with a certain LOS path step. The slope of straight-line path S_t between antenna and target is calculated in a similar way:

$$S_t = \frac{h_t - h_r}{d_p}, \quad (4.2)$$

where h_t is target height AMSL in meters, h_r is radar antenna height AMSL in meters, and d_p is earth path distance between the radar and the target in kilometers. Earth's bulge is not included here since it is relative to the path itself and is therefore the same as with the radar. The radar's visual horizon is defined as a point on the entire profile that has the greatest slope. However, if some slope S_i is greater than the slope S_t the terrain

is above the LOS path and the propagation method is therefore transhorizon. As such, the LOS path diffraction at some coordinates i is dependent on S_i and on S_t .

4.2 Diffraction modeling of radio wave propagation

Determining the diffraction model comes down to knowledge of obstacles and the terrain. The decision of which model to use should be based on the dominant terrain points along the propagation path and the extent to which they interfere with the radio signal. The methodology of acquiring this information along the propagation path is described in previous Section 4.1. A terrain profile defines the way of radar signal propagation. To estimate diffraction loss caused by encountered natural obstacles, it is necessary to idealize their form. Under some circumstances, a dominant terrain can be assumed as a bold smooth obstacle with a well-defined radius of curvature at the top. However, most of the time it is more reasonable to assume a knife-edge of negligible thickness. Choosing a diffraction model in this method is simplified with a flow chart in Figure 4.2.

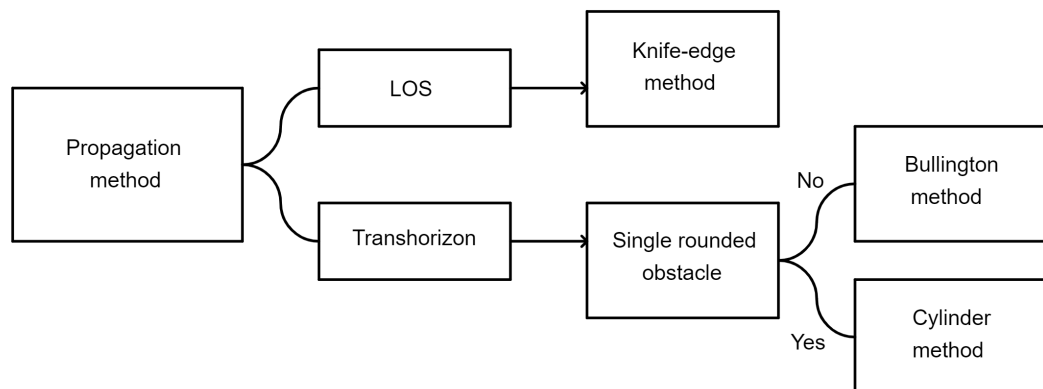


Figure 4.2. The flow chart for choosing a diffraction model based on a elevation profile of a propagation path.

If any terrain point along the propagation path rises above the straight-line path from the radar to the target, causing the target to be below the radar's horizon, it is interpreted as a trans-horizon propagation. As a result, several obstacles along the terrain profile between the radar and the target may cause diffraction to the transmitted signal. The Bullington diffraction model is chosen whenever the visual horizon is being blocked. Its usage is described in Section 2.7.

In case of LOS propagation, the diffraction loss is calculated only from the most dominant obstacle with KED. The model considers only the most dominant obstacle in the signal path, as this will typically have the greatest impact on the path loss. Furthermore, considering multiple obstacles in the path of the radio wave can significantly increase the

complexity of the path loss calculation leading to increased computational requirements. The profile point that interacts with the first Fresnel zone the most is seen as a dominant. To find the single most dominant profile point, from the perspective of the simulated radar, their capabilities to intervene with the signal's Fresnel zones have to be evaluated. This is done by calculating the Fresnel diffraction parameter ν , from Eq. 2.5, for each profile point. The dominant profile point is the one with the highest parameter value.

Since the terrain model is not accurate enough to provide information about the appearances of singular natural objects such as small hills, the usage of the rounded obstacle model should be considered for each situation separately. It may be used on medium-sized hills with a smooth surface and a known radius. This model allows for the calculation of increased diffraction loss resulting from the rounded characteristics of an obstacle, as opposed to assuming there was a knife-edge. The model has same first prerequisite as the Bullington model; propagation has to be trans-horizon. In addition, terrain above the straight-line path has to have a rounded shape but also separate horizon points of the radar and the target with their distance not too far away from each others. The terrain type of a dominant terrain has to have certain characteristics. For example, with trees or buildings present, no actual cylinder can be fit into the terrain profile. For those obstacles where usage of the model is justified, a cylinder radius can be calculated with equations provided by ITU-R P.526 [10].

4.3 Summary of methods

The main objective was to develop a methodology to flexibly express any ground-based surveillance radar as a digital twin with which the surrounding terrain's effect can be modeled. In this chapter, the focus was on methods used to incorporate different types of geospatial information, including ground elevation data and vegetation height data, into calculating propagation path diffraction caused by terrain obstacles between two coordinate points. The methodology is divided into two sections. In the first Section 4.1, data matrices were mapped by defining coordinates for each pixel, and their AER positions are determined relative to the radar while taking into account signal refraction. The pixel azimuths were then compared to the azimuth direction of the target, and the pixels that had the smallest difference were identified as being under the LOS path. The present procedure works regardless of the grid size of geospatial materials, making it more flexible in its use with other terrain materials. Moreover, it affords the flexibility to selectively choose pixels from the data by setting different function inputs. This is beneficial when diffraction models other than those adopted in this work need to be used. In the second Section 4.2, the combined model was created for making a logical decision between diffraction models based on properties of the propagation path. Because the elevation profile is determined in advance, decision-making between diffraction models is straight-

forward, and the diffraction loss can be calculated from the height values, which makes the process computationally fast and increases the digital twin modularity.

5. RESULTS

This chapter displays the results obtained using the digital twin presented previously in Chapter 4, demonstrated through visualization for five different cases. The path attenuation due to the diffraction was calculated to multiple locations at the same time. The loss caused by each terrestrial path, was calculated one way, from the radar to each target. Targets were set as a large grid around the radar for each different case to demonstrate the terrain's effect on the attenuation loss as the signal traveled further away from the radar site. The grid was set to reach the range of 150 kilometers in every direction with a grid size of 5 km x 5 km. Loss caused by factors other than path attenuation due to terrain's diffraction, including free space loss, are not presented. Table 5.1 presents a summary of each case, including the Case ID, the target grid height in meters, which diffraction model is being used, is the vegetation data applied, and the corresponding result figure. In case 3, the radar signal's interference with the terrain is examined without vegetation data since its density and form may vary and classical diffraction models do not accurately apply propagation paths through them. Although there are models for diffraction caused by vegetation [28] [32], they are not universal, and therefore the vegetation is treated as an obstacle.

Case ID	Target height (m)	Model used	Vegetation	Result figure
1	500	KED	Yes	5.1
2	500	Combined	Yes	5.2
3	500	KED	No	5.5
4	1000	KED	Yes	5.7
5	1000	Combined	Yes	5.8

Table 5.1. Result cases.

The chosen radar site for this scenario is located in southern Finland on 60°71'32" North and 24°08'63" East in the WGS84. The ground there lies at an altitude of 184 meters AMSL, and the antenna is 12 meters Above Ground Level (AGL). It should be noted that this site for the radar's digital twin was selected for demonstration purposes due to its relatively high ground elevation in the region. Vegetation is cut down to a distance of 50 meters in every direction to create a more realistic scenario for the site. Similar to the other input parameters, the step size is set to 25 meters and Nearest Neighbor (NN)

value is set to 1 for this radar. In this way, only the terrain map values just along the propagation path are being utilized. Every diffraction model used in these results simplifies the terrain into a one-dimensional edge, represented by a vertical red line. The scale of path attenuation was clipped to 20 dB to achieve more reasonable values for a radar's use-case. If the scale had been chosen to represent all loss values, most of the figures would be dominated only by the two opposite colors. In trans-horizon propagation, diffraction losses will easily grow tenfold which would make propagation paths just above the ground unrecognizable with this kind of scale. Outcomes of the digital twin are qualitative, but no ground truth exists, so they should be viewed in that regard.

5.1 Case 1

At first, diffraction loss is calculated just from the most dominant obstacle by using the KED as seen in Figure 5.1. The visual paths from the radar to the targets in the northeast and southwest are being blocked by nearby trees, despite the reduction of all vegetation to 50 meters from the site. The target grid is located at a height of 500 meters AMSL. With the KED model, the dominant terrain is determined not by the largest slope, but by the point that has the most interference with the Fresnel zone.

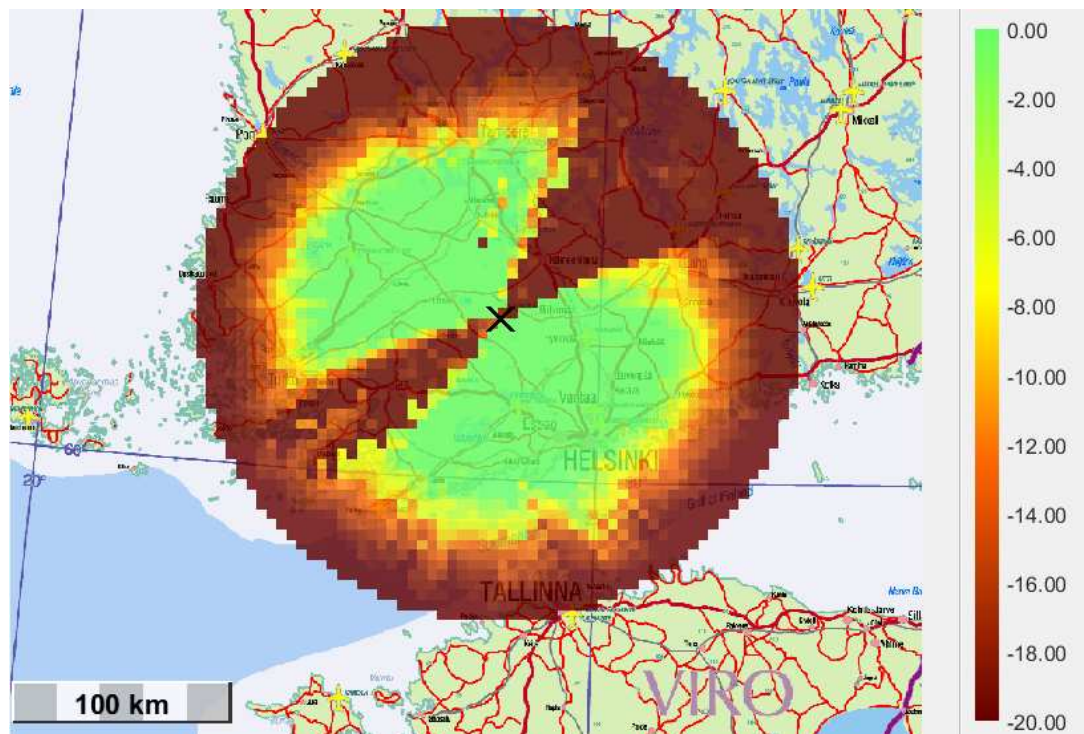


Figure 5.1. Case 1. The path attenuation by the most dominant terrain point to targets at 500 meters AMSL using KED.

5.2 Case 2

The combined model, introduced in Section 4.2, is used in this case, as presented in Figure 5.2. The scenario is the same as in the previous case. The only difference between the two cases is the model used to calculate trans-horizontal targets. By comparing these two cases, there is no significant difference in loss values as measured by this decibel spectrum. The small difference for the first two cases in terms of attenuation demonstrates the significance of the first dominant obstacle. The most visible difference can be seen in the southwest. If the propagation path has some other dominant terrain points, the combined model will be more precise. This, of course, requires the target to be behind several terrain points. Therefore, only obstacles behind the first dominant terrain with significant height will have this increasing effect.

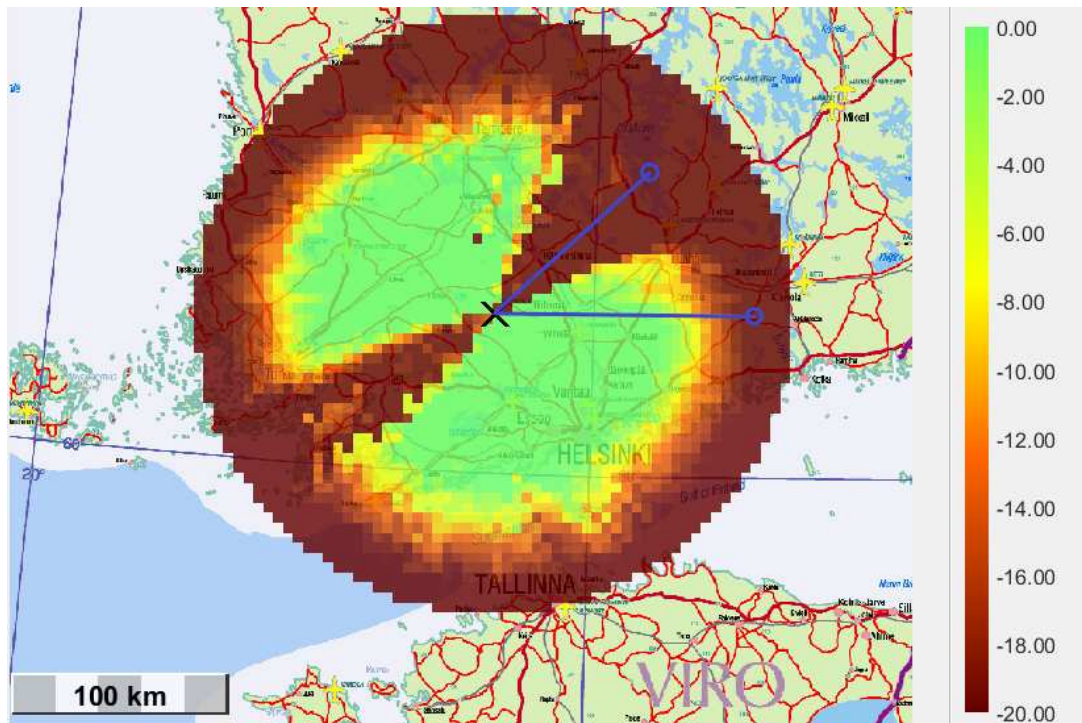


Figure 5.2. Case 2. The path attenuation to targets at 500 meters AMSL using the combined model. Blue lines indicate propagation paths. Terrain cross-section of path to northeast is shown in Figure 5.3 and path to east in Figure 5.4.

If the radar's visual horizon is not limited by an immediate obstacle near the sensor site the curvature of the Earth will usually have significantly more impact on determining that horizon. When the angle to a target is large, the positive curvature of the Earth might cause terrain to obstruct the propagation path even if that obstacle is not significantly higher than the terrain before it. On the contrary, negative curvature might make distant obstacles irrelevant for calculating the diffraction. This phenomenon is shown in Figure 5.3, where the propagation path to the target is instantly blocked by trees near the radar. Additionally, the edge, determined using the Bullington model, rises remarkably high,

causing an attenuation of over 30 decibels. The effect of the curvature can also be seen by comparing Figures 5.2 and 5.8 when target is moved up from 500 to 1000 meters.

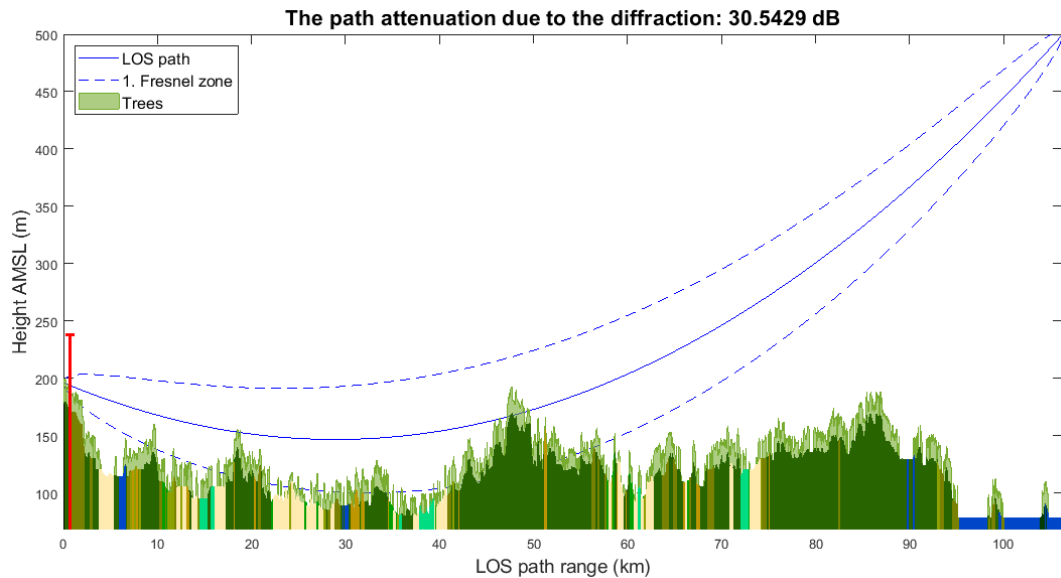


Figure 5.3. Case 2 - Fig. 5.2. Terrain under the propagation path to the target in north-east at 500 meters AMSL. The red vertical line describes the knife-edge defined by the Bullington model.

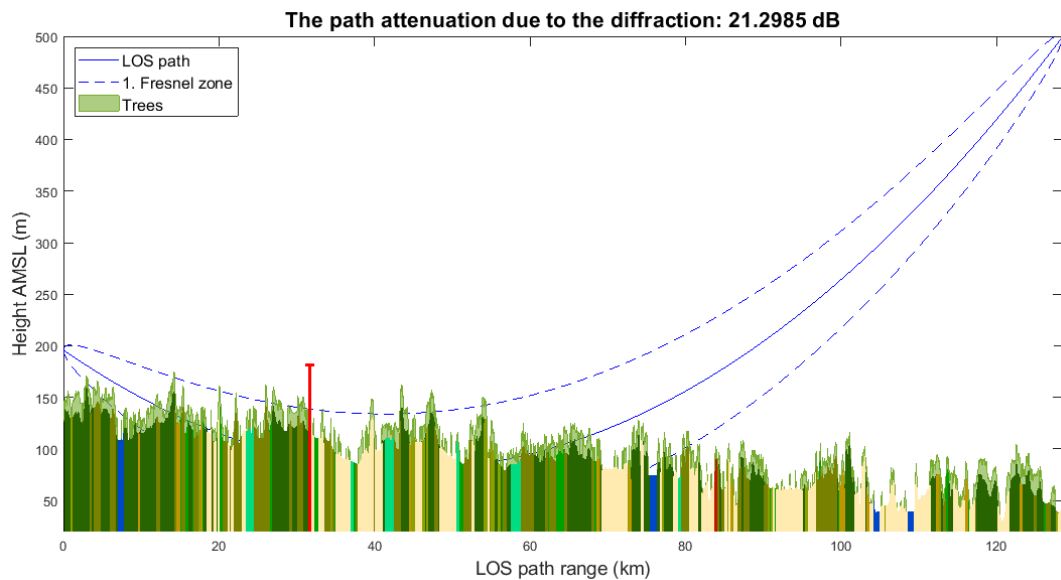


Figure 5.4. Case 2 - Fig. 5.2. Terrain under the propagation path to the target in east at 500 meters AMSL. The red vertical line describes the knife-edge defined by the Bullington model.

5.3 Case 3

To demonstrate the effect vegetation has on diffraction loss, it is removed completely, as demonstrated in Figure 5.5. The basis is otherwise the same as in the Case 1 and the loss is calculated with KED diffraction by the most dominant obstacle. The most remarkable difference can be seen in northeast and in southwest directions, where the radar signal is no longer interfered with by the optical horizon defined by the trees near the sensor. A cross-section of the same terrain under the path to the Northeast, with no vegetation, can be seen in Figure 5.6. This is similar to the cross-section shown in Figure 5.3. Although the LOS is still being blocked within this range, the loss due to diffraction has significantly decreased. The target is more likely to be detected, as the loss due to diffraction has decreased significantly from over 30 dB to 6.2 dB. It is reasonable to conclude that the actual loss would fall within the range of these two values, as vegetation cannot be entirely disregarded and at the same time, it cannot be accurately represented as an impenetrable edge.

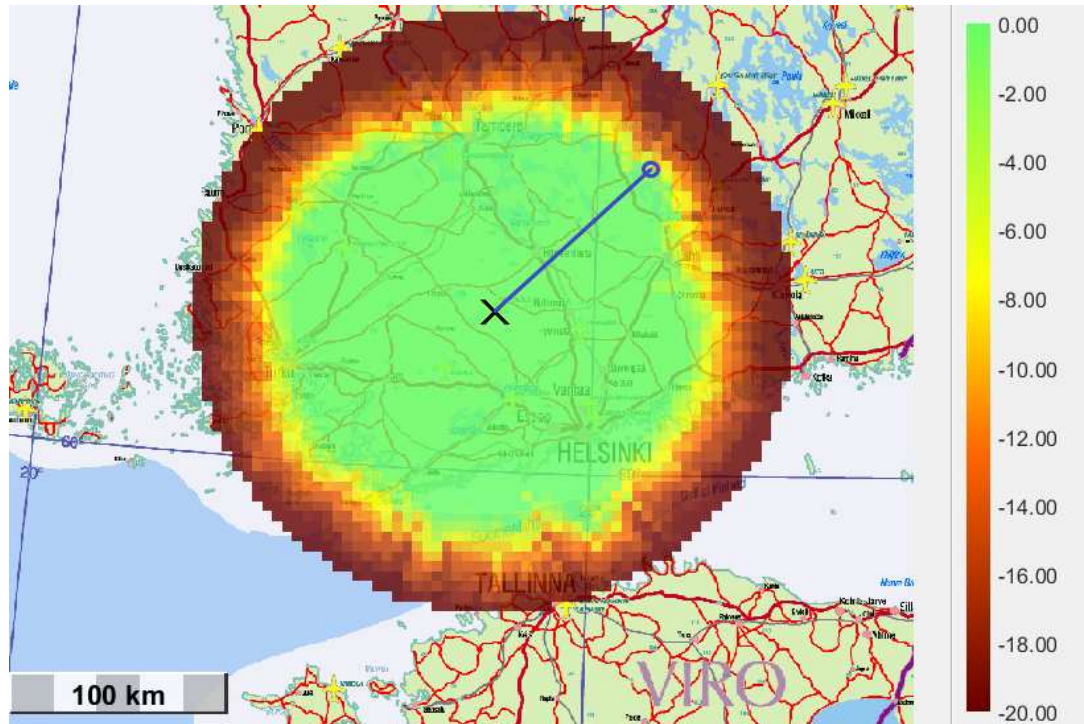


Figure 5.5. Case 3: The path attenuation by the most dominant terrain point without vegetation to targets at 500 meters AMSL using KED. The blue line indicate propagation path to northeast. Terrain cross-section of the path is shown in Figure 5.6

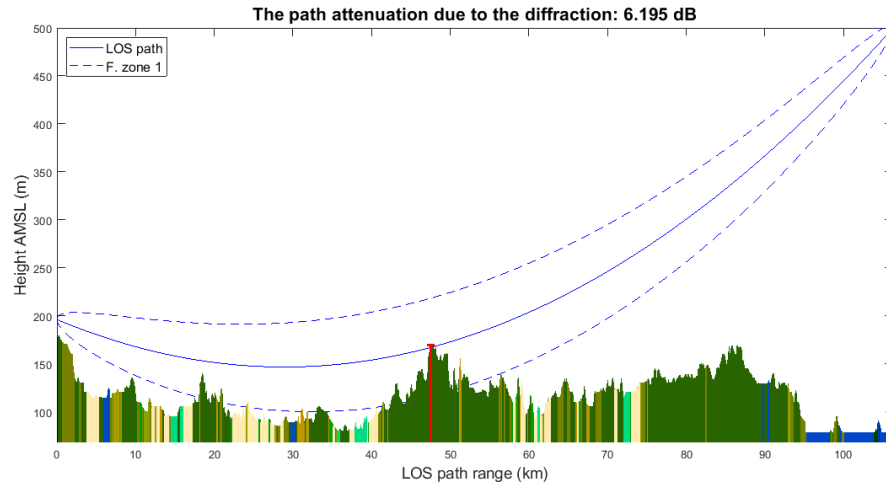


Figure 5.6. Case 3 - Fig. 5.5. Terrain under the propagation path to the target in northeast without vegetation. The red vertical line describes the knife-edge defined by the KED model.

5.4 Case 4

For Case 4 and 5, the target grid is set higher at an altitude of 1000 meters AMSL. In this case, as in Case 1, only the KED model is used. As can be seen from Figure 5.7, the attenuation is reduced at longer distances compared to the previous target grid that was at a lower altitude. The negative impact from earth's positive curvature is reduced since propagation path travels high enough. In addition, the positive curvature is also quite insignificant at these distances. What can be also noticed is that the effect of the terrain near the sensor is emphasized even more with relatively flat terrain. This can be seen in Figure 5.9.

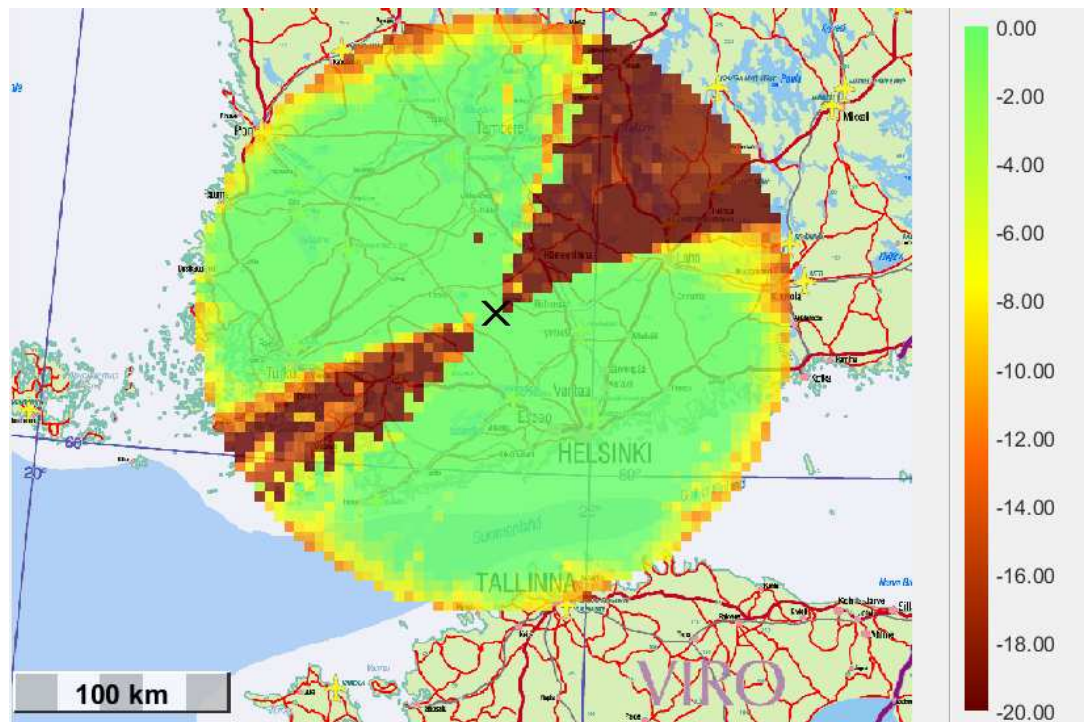


Figure 5.7. Case 4: The path attenuation by the most dominant terrain point to targets at 1000 meters AMSL using KED.

5.5 Case 5

This case demonstrates how the combined model works once terrain intervenes less with the radar signal. However, relatively flat terrain causes the KED model to be used most of the time with combined model since no other obstacles rise in immediate vicinity of the signal. This is because the positive curvature of the Earth is not large enough when the signal travels at higher altitudes. This can be seen by comparing the cone in the previous case, as presented in Figure 5.7, to the one in this case, found in Figure 5.8. The difference can also be illustrated by comparing the terrain cross-section in Figure 5.3 to one in Figure 5.9. On the other hand, when the Bullington model is used in a given situation, the edge is typically defined in close proximity to the sensor. Despite the use of trans-horizon propagation method, the obtained results using this model are often similar to those achieved using the KED model. This means that the Bullington model is defined by the same optical horizon point from both sides as seen in Figure 5.9.

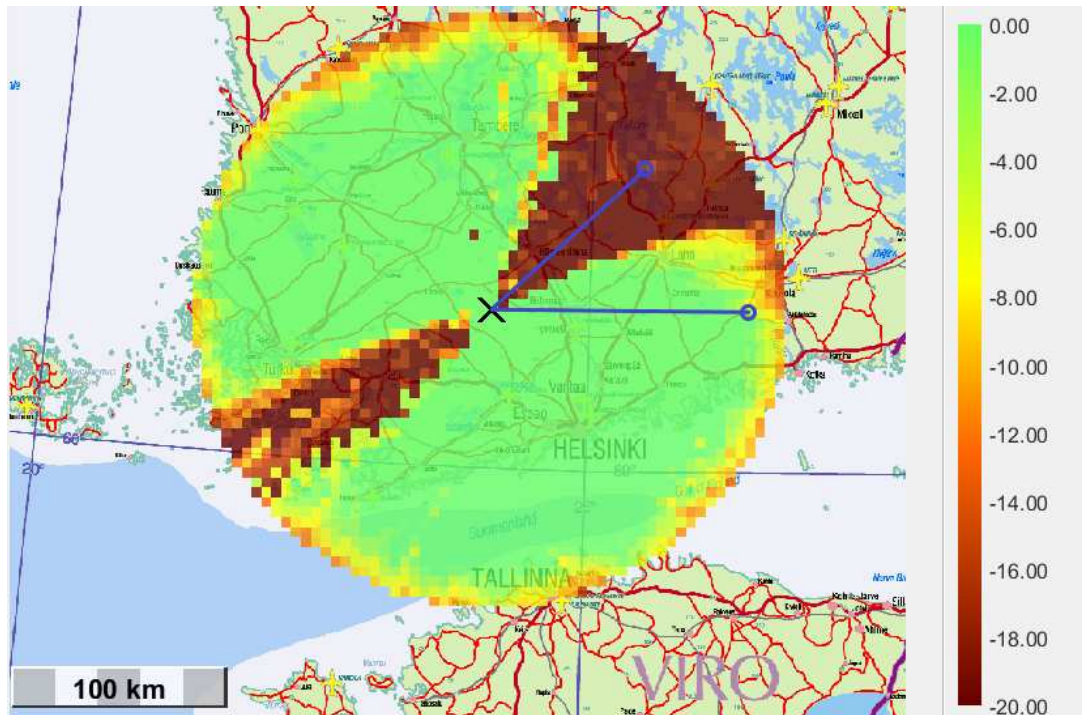


Figure 5.8. Case 5: The path attenuation to targets at 1000 meters AMSL using the combined model. Blue lines indicate propagation paths. Terrain cross-section of path to northeast is shown in Figure 5.9 and path to east in Figure 5.10.

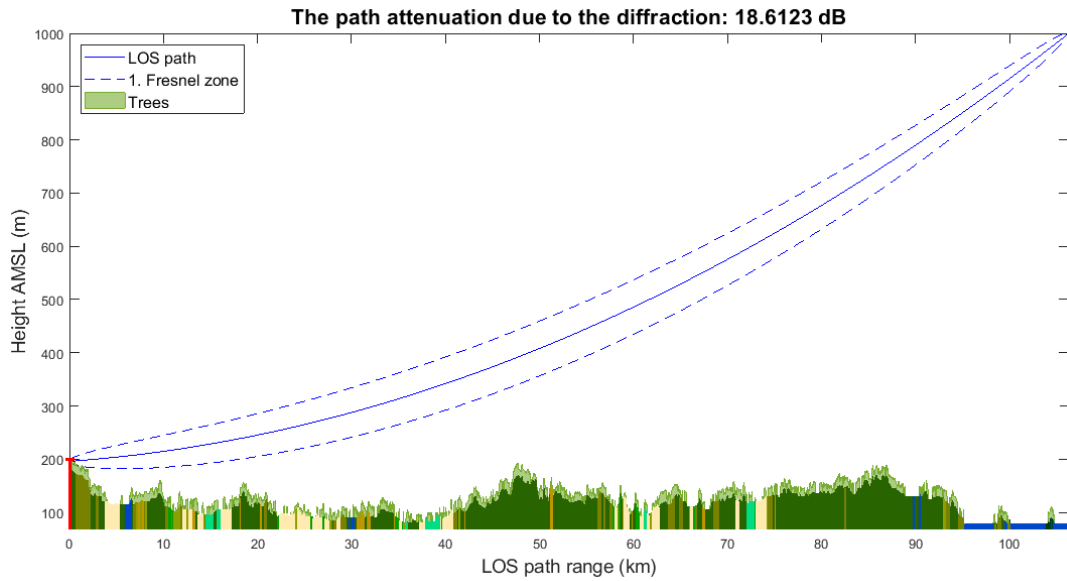


Figure 5.9. Case 5 - Fig. 5.8. Terrain under the propagation path to the target in north-east at 1000 meters AMSL. The red vertical line describes the knife-edge defined by the Bullington model.

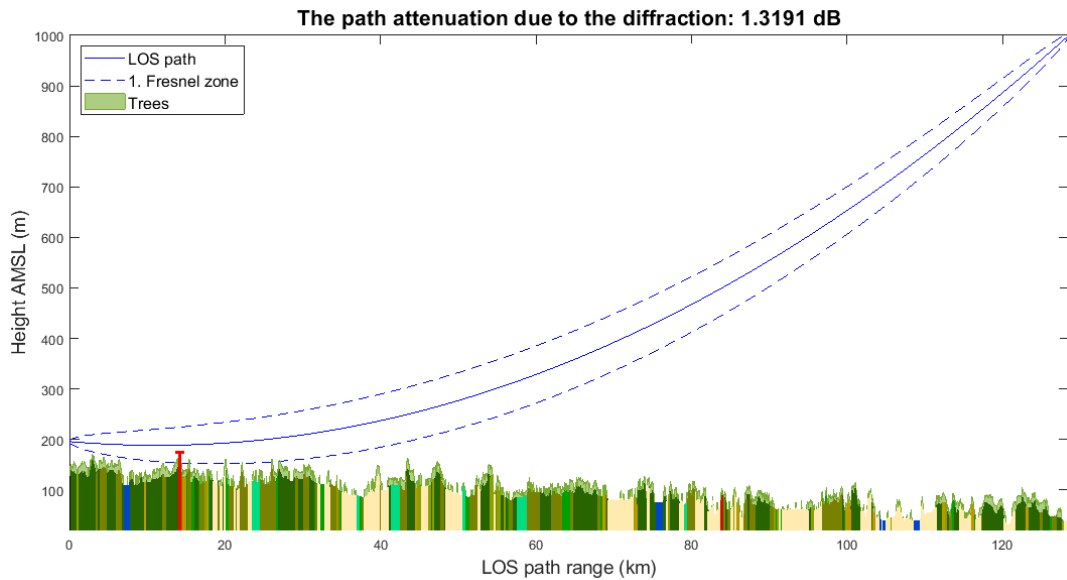


Figure 5.10. Case 5 - Fig. 5.8. Terrain under the propagation path to the target in east at 1000 meters AMSL. The red vertical line describes the knife-edge defined by the KED model.

5.6 Summary of results

The aim of these digital twin simulation cases was twofold: firstly, to compare different diffraction models and their results in the context of a ground-based surveillance radar, and secondly, to evaluate the use of a combined diffraction model. Both the KED and Bullington models provide simple yet similar ways to calculate the volume of attenuation due to diffraction without specifying the type or form of the obstacle. The loss scale used in the results was chosen to represent the most interesting range of attenuation values for a radar system in decibels. The results of the loss value measurements are quantitative, but they should be interpreted as qualitative rather than definitive. This is because obstacles, both the ground irregularities and vegetation, are modeled as simple 1-D edges, which may not precisely reflect real-world objects. Nevertheless, the results were consistent with theoretical expectations. Moreover, this thesis demonstrates the potential of the proposed methodology for future research and practical applications.

For terrain with relatively small height differences the curvature of the Earth might have a significant impact on limiting the radar coverage. The elevation slope from a radar to the target, as well as from a radar to individual terrain points along the path to a target, therefore plays a large role in defining the degree of diffraction. It can be derived from the target height divided by its distance from the radar site. For example, if the target height remains constant, the curvature begins to cause problems as the target moves further away. In some cases, the radar antenna may be located at a lower level than the vegetation surrounding the site. In such case, the radar's visual horizon and detection ability can be greatly improved by reducing this vegetation.

6. DISCUSSION AND CONCLUSION

The objective of this thesis was to develop a methodology for representing a ground-based surveillance radar as a digital twin and to evaluate its performance based on the amount of diffraction caused by the terrain. This was achieved by calculating the attenuation caused by natural obstacles surrounding the radar site in different directions and altitudes. The calculations were based on knowledge of the ground topography, tree heights, and type of land coverage. Three main diffraction models were considered to model the obstacles as edges with a certain height but infinite width. The Knife-Edge Diffraction (KED) model simplifies an object as a one-dimensional edge or wall with infinite width. It was used in Line-of-sight (LOS) propagation scenarios to calculate diffraction from the terrain point interacting the most with the propagation path. In trans-horizon propagation scenarios, the Bullington model was implemented. This model simplifies all the terrain above the LOS path into a single knife-edge. The knife-edge is defined by the extensions of the visual horizons of both the radar and the target. In addition, the rounded obstacle model was considered to be applied. This model is generally used to calculate diffraction from obstacles with smooth characteristics and requires the target to be under the visual horizon of the radar. However, the rounded obstacle diffraction model is not suitable for environments dominated by forests and varying terrain heights. It is better suited for single and smooth hilltops, which upward-looking surveillance radars rarely encounter. Another challenge was the accuracy of the data, which did not provide possibility to model terrain in a way that would enable visualization of certain shapes. As a result, only the KED and Bullington models were used in this work.

While these diffraction models are generally useful and satisfactory in most scenarios, they have certain limitations. One of these limitations is that they assume obstacles as simple 1-D edges, which may not accurately reflect real-world objects. Therefore, the results of these models may not always be entirely accurate, and more advanced modeling techniques may be necessary to capture the full complexity of the terrain. In addition, while the results were still in line with the theory, the geospatial data offered some challenges for implementing more accurate models. False interpretation of terrain may cause error in calculated dimensions. The better the accuracy of the ground elevation and forest height data, the easier it is to justify the use of the chosen diffraction model. The used forest height data, containing information about maximum tree heights, is satisfac-

tory for estimating the greatest possible diffraction. However, interpreting the vegetation as an edge may not be suitable for calculating the diffraction. With current methods, the diffraction from obstacles including at least some vegetation should be observed with and without it, as the truth could be somewhere between these two results. The land cover data used in this work has smaller spatial accuracy compared to the height data materials. It also lacks information about some smaller but still dominating features of the terrain, such as cliffs and large erratic boulders. Nonetheless, it is useful to include that data as a reference when reporting the environment from which the diffraction loss value is calculated.

It is challenging to accurately predict the magnitude of signal diffraction from the tip of an obstacle when the vertical dimension of the obstacle cannot be adequately modeled in despite of which diffraction model is being used. Obstacles near the radar antenna, especially the ones that are horizontally tapering such as an esker, might cause more error due to inaccuracies in geospatial data. One way to improve the proposed methodology instead of describing terrain obstacles as 1-D edges is to model them in 2-D by also including the horizontal dimension. The diffraction could be then calculated with Fresnel-Kirchhoff model described in Section 2.8. However, this would also require more accurate geospatial data to be performed. Another approach that could also improve diffraction modeling would be the better exploitation of land coverage type data. For example, while the tree data gives out the heights of the vegetation, this data could be used together with more sophisticated diffraction models for calculating the attenuation based on other features of the vegetation. However, the problem is the lack of such models which limits the exploitation of land type data.

The techniques for calculating diffraction from a particular location to surrounding terrain points using various geospatial data sets, such as a Digital Elevation Model (DEM) [13], or choosing a diffraction model based on path profile analysis [10], are established methods. However, the use of a digital twin in the context of a radar system was not widely adopted until recent years [27] [33]. Although the concept of modeling radar performance with natural obstacles is not new, its application within the context of a site-specific digital twin appears to be less studied. Specifically, the diffraction loss caused by the most dominant natural obstacles in the surrounding terrain of a radar site has not been studied within the framework of a digital twin. In most cases, the path attenuation caused by diffraction of the terrain can simplify the obstacles enough to be used as one indicator of radar system performance with the current data and diffraction models. However, it is important to acknowledge the limitations of the current methods presented in this work and to conduct further research to address them. At this stage, the results should be considered indicative rather than definitive due to some unknown characteristics of the terrain. The total performance of a radar system consists of multiple factors, and this work only focused on the effect of surrounding terrain.

REFERENCES

- [1] S. Watts, H. Griffiths, J. Holloway, A. Kinghorn, D. Money, D. Price, A. Whitehead, A. Moore, M. Wood, and D. Bannister. *The specification and measurement of radar performance*. IET, 2002.
- [2] M. Talbot-Smith. “8 - Sound, speech and hearing”. *Telecommunications Engineer’s Reference Book*. Ed. by F. Mazda. Butterworth-Heinemann, 1993, pp. 8-1-8–16.
- [3] C. Wolff. *Radartutorial.eu*. 1998. URL: <https://www.radartutorial.eu/index.en.html> (visited on 02/10/2023).
- [4] J. C. Whitaker. *The Electronics Handbook*. CRC Press, 1996, p. 1321.
- [5] ITU-R P.525-4. *Calculation of free-space attenuation*. Standard. Geneva: International Telecommunication Union, 2019. URL: <https://www.itu.int/rec/R-REC-P.525/en>.
- [6] *Line of Sight Obstruction*. Campbell Scientific, Inc., 2016.
- [7] M. A. Richards. *Principles of Modern Radar*. Vol. Volume I - Basic Principles. SciTech Publishing, Inc., 2010.
- [8] B. B. Baker and E. T. Copson. *The mathematical theory of Huygens’ principle*. Vol. 329. American Mathematical Soc., 2003.
- [9] L. Barclay. *Propagation of Radiowaves*. 3rd ed. London, UK: Institution of Engineering and Technology, 2013.
- [10] ITU-R P.526-15. *Propagation by diffraction*. Standard. Geneva: International Telecommunication Union, 2019.
- [11] L. Vogler. *Further Investigations of the Multiple Knife-Edge Attenuation Function*. U.S. Department of Commerce, 1983.
- [12] B. Arbesser-Rastburg. *Radiowave Propagation Information for Designing Terrestrial Point-to-Points Links*. International Telecommunication Union, 2008.
- [13] D. J. Breton. *A Study on the Delta-Bullington Irregular Terrain Radiofrequency Propagation Model*. The U.S. Army Engineer Research and Development Center (ERDC), 2022.
- [14] Y. Xu, Q. Tan, D. Erricolo, and P. Uslenghi. “Fresnel-Kirchhoff integral for 2-D and 3-D path loss in outdoor urban environments”. *IEEE Transactions on Antennas and Propagation* 53.11 (2005), pp. 3757–3766.
- [15] P.Pertilä. “A Parametric Wind Turbine Model using Fresnel Diffraction (in preparation)”. (2023).
- [16] J. H. Whittaker. “Fresnel-Kirchhoff theory applied to terrain diffraction problems”. *Radio Science* 25.05 (1990), pp. 837–851.

- [17] A. Ghasemi, A. Abedi, and F. Ghasemi. *Propagation engineering in wireless communications, 2nd edition*. Springer, 2012.
- [18] H.-J. Li and Y.-W. Kiang. “10. - Radar and Inverse Scattering”. *The Electrical Engineering Handbook*. Ed. by W.-K. Chen. Burlington: Academic Press, 2005.
- [19] G. M. Brooker. *Conical-Scan Antennas for W-Band Radar Systems*. Australian Centre for Field Robotics, University of Sydney, 2003.
- [20] H. Kuschel, D. Cristallini, and K. E. Olsen. “Tutorial: Passive radar tutorial”. *IEEE Aerospace and Electronic Systems Magazine* 34 (2019).
- [21] S. H. Javadi and A. Farina. “Radar networks: A review of features and challenges”. *Information Fusion* vol. 61 (2020).
- [22] J. B. Billingsley. *Low-Angle Radar Land Clutter: Measurements and Empirical Models*. 2002.
- [23] H. Dale. *A Comparison of Convolutional Neural Networks for Low SNR Radar Classification of Drones*. Institute of Electrical and Electronics Engineering (IEEE), 2021.
- [24] Y. S. Meng. *The Effects of Tropical Weather on Radio-Wave Propagation Over Foliage Channel*. Institute of Electrical and Electronics Engineering (IEEE), 2009.
- [25] T. Thayaparan, D. Dupont, Y. Ibrahim, and R. Riddolls. “High-Frequency Ionospheric Monitoring System for Over-the-Horizon Radar in Canada”. *IEEE Transactions on Geoscience and Remote Sensing* 57.9 (2019).
- [26] D. Jones, C. Snider, A. Nassehi, J. Yon, and B. Hicks. “Characterising the Digital Twin: A systematic literature review”. *CIRP Journal of Manufacturing Science and Technology* 29 (2020).
- [27] T. Rouffet, J.-B. Poisson, V. Hottier, and S. Kemkemian. “Digital twin : a full virtual radar system with the operational processing”. *2019 International Radar Conference (RADAR)*. 2019.
- [28] ITU-R P.833-10. *Attenuation in vegetation*. Standard. Geneva: International Telecommunication Union, 2021. URL: <https://www.itu.int/rec/R-REC-P.833/en>.
- [29] *Maps and spatial data*. National Land Survey of Finland. 2022. URL: <https://www.maanmittauslaitos.fi/en/maps-and-spatial-data> (visited on 09/14/2022).
- [30] S. Bontemps and O. Arino. *Globover 2009, Products Description and Validation Report*. Tech. rep. European Space Agency (ESA), 2011. URL: https://epic.awi.de/id/eprint/31014/16/GLOBCOVER2009_Validation_Report_2-2.pdf.
- [31] M. Ollikainen, ed. *The Finnish Coordinate Reference Systems*. the National Land Survey of Finland and the Finnish Geodetic Institute, 2016.
- [32] Y. Zheng, ed. *6. - Radio Wave Propagation Through Vegetation*. 2013.
- [33] M. Klein, T. Carpentier, E. Jeanclaude, R. Kassab, K. Varelas, and N. de Bruijn. “AI-Augmented Multi Function Radar Engineering with Digital Twin: Towards Proactivity”. (2020).